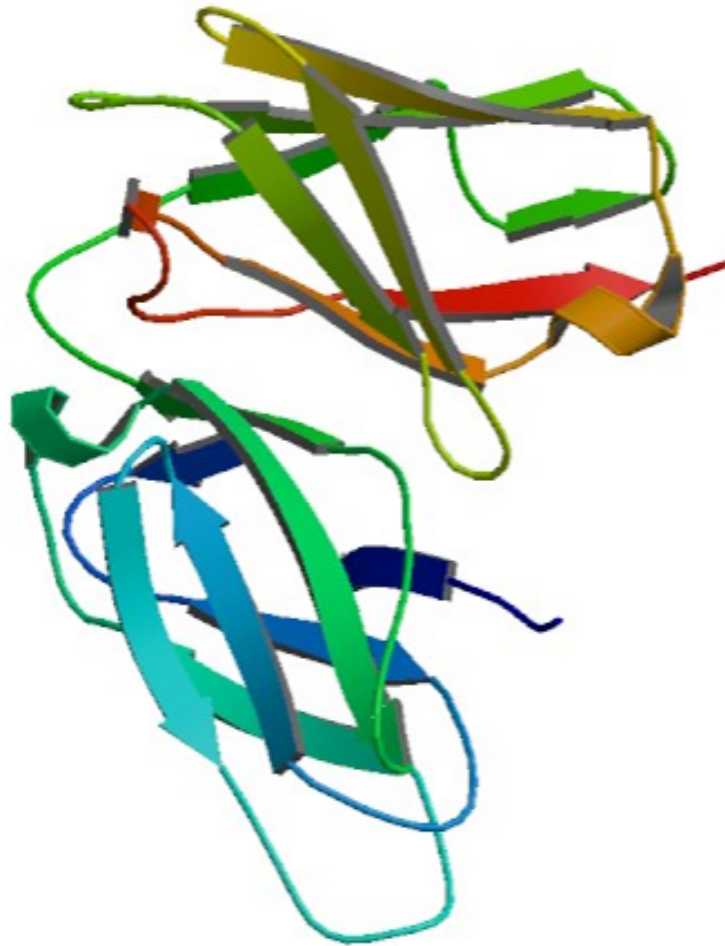




CHALMERS
UNIVERSITY OF TECHNOLOGY



A CRISPR approach to manipulating NK cell receptor ligand expression in leukemic cells

Master's thesis in Biotechnology
Linnea Kristenson

MASTER'S THESIS 2018

**A CRISPR approach to manipulating
NK cell receptor ligand expression
in leukemic cells**

LINNEA KRISTENSON



CHALMERS
UNIVERSITY OF TECHNOLOGY

Department of Biology and Biological Engineering
CHALMERS UNIVERSITY OF TECHNOLOGY
Gothenburg, Sweden 2018

A CRISPR approach to manipulating NK cell receptor ligand expression
in leukemic cells
LINNEA KRISTENSON

© LINNEA KRISTENSON, 2018.

Supervisor: Fredrik Bergh Thorén, Department of Infectious Diseases at Institute
of Biomedicine
Examiner: Christer Larsson, Department of Biology and Biological Engineering

Master's Thesis 2018
Department of Biology and biotechnology
Chalmers University of Technology
SE-412 96 Gothenburg
Telephone +46 31 772 1000

Cover: Structure of the human natural cytotoxicity receptor NKp46.
Obtained from rcsb.org, deposited by Foster, C.E., Colonna, M., Sun, P.D.

Typeset in L^AT_EX
Gothenburg, Sweden 2018

A CRISPR approach to manipulating NK cell receptor ligand expression
in leukemic cells

LINNEA KRISTENSON

Department of Biology and Biotechnology

Chalmers University of Technology

Abstract

Natural killer (NK) cells are important innate lymphocytes in the immune system and have been considered to be vital in fighting cancer, virus infections as well as regulating immune responses. The activity of NK cells is regulated via a complex signaling between inhibitory and activating receptors. Ligands for most of the activating receptors have been discovered but no endogenous ligand for one of the important natural cytotoxicity receptors, NKp46 has been identified. Therefore, the long term aim of this thesis project was to define ligand candidates for the activating receptor NKp46 with intermediate aims to manipulate expression of NK cell activating receptor ligands in the K562 cell line using a CRISPR approach.

The result from the performed cytotoxicity assays demonstrated the importance of the activating receptors NKp30 and DNAM-1 in elimination of K562 cells and the expression of the complementary ligands NCR3LG1, PVR and NECTIN2 was confirmed using RT-qPCR. The successful creation of a Cas9-expressing K562 cell line was demonstrated, including verification of Cas9 protein expression using both flow cytometry and western blot. Following that, a constructed plasmid with the gRNA for the B7-H6 gene, NCR3LG1, was generated and shown to create a cleavage and mutation within the gene. The engineered cell line was ultimately shown to have a reduced expression of the B7-H6 protein, indicating the successful knockout of the NCR3LG1 gene.

Keywords: Natural killer cells, NKp46, leukemia, flow cytometry, CRISPR/Cas9, Western blot, RT-qPCR, lentiviral vector, K562 cell line.

Acknowledgements

The year I have spent at the third floor at Sahlgrenska Cancer Center has been an exciting time and in many ways different from the previous studies. I want to thank everyone that have helped me in and around the lab.

I especially want to thank my supervisor Fredrik Bergh Thorén, who gave me the opportunity to run this intriguing project and has supported me with guidance and lots of encouragement throughout this year.

Ka-Wei Tang has shared his knowledge in everything related to plasmid cloning and gRNA design which has been invaluable to me.

Alexander Hallner and Elin Bernson have helped me a lot in the lab and especially with the flow cytometer.

Malin Nilsson was very pedagogical when she helped me with the RT-qPCR experiments, Ali Akhiani took the time to explain everything in connection to the western blot procedure and Roberta Kiffin and Yarong Tian showed great support in helping me with my plasmid-related questions.

I also want to thank Ebru Aydin for being a great desk mate.

Finally, I want to thank my boyfriend Fredrik Nyhlén and my family for always being supportive and believing in me.

Linnea Kristenson, Gothenburg, May 2018

Contents

List of Figures	xi
List of Tables	xv
List of Abbreviations	xvii
1 Introduction	1
1.1 Aim	1
1.2 Clarification of the issue under investigation	2
2 Theory	3
2.1 The immune system	3
2.1.1 Innate immune system	3
2.1.2 Adaptive immune system	4
2.2 Natural Killer Cells	5
2.2.1 The "missing self" theory	5
2.2.2 Inhibitory NK cell receptors	6
2.2.3 Activating NK cell receptors	7
2.3 Cell lines	7
2.4 Flow cytometry	7
2.5 Cytotoxicity Assay	9
2.6 RT-qPCR	10
2.7 CRISPR/Cas9	11
2.8 T7 Endonuclease I Assay	11
3 Methods	13
3.1 Culture conditions	13
3.2 Cell separation and NK cell cytotoxicity	13
3.3 RT-qPCR	16
3.4 Lentiviral transduction of K562 cells	17
3.5 Cas9 staining	17
3.6 Western Blot	18
3.7 gRNA design	19
3.8 Plasmid construction	19
3.9 gRNA transfection of K562 cell line	21
3.9.1 Analysis of transfection efficiency and viability	21
3.9.2 T7 Endonuclease I assay	21

3.9.3	B7-H6 and PVR staining	22
4	Results & Discussion	23
4.1	NK cell cytotoxicity	23
4.2	Ligand expression using RT-qPCR	24
4.3	Blasticidin experiments	26
4.4	Verification of Cas9 expression	27
4.4.1	Flow cytometry	27
4.4.2	Western blot	28
4.5	gRNA design	28
4.6	Verification of gRNA transfection	30
4.7	Verification of functional Cas9 and cleavage of genes	32
4.8	Verification of reduced expression of B7-H6 and PVR	33
5	Conclusion	39
	Bibliography	41
A	Appendix 1	I
A.1	Primers	I
A.2	Designed gRNA insert sequence	II
A.3	crRNA oligomers	II
B	Appendix 2	III
B.1	RT-qPCR programs	III
B.2	Spinoculation protocol	III
B.3	Annealing of oligomers	IV
B.4	Combined digestion and ligation	IV
B.5	PCR program for B7-H6 and PVR	V

List of Figures

2.1	<i>Difference in recognition mechanism between T cells and NK cells. a) Normal cells expressing MHC class I molecules with bound self-peptides are resistant to both lymphocytes. T cells recognize the MHC class I molecule that presents viral peptides, b), but fail to detect infected cells with downregulated MHC class I c). Instead NK cells do not generally discriminate between self and viral peptides but rather the expression of MHC class I itself, which is shown in b) and c). Virus B evades T cell detection due to downregulation of MHC class I, which is instead recognized by the NK cell, resulting in target cell lysis.</i>	6
2.2	<i>Flow cytometry schematic. Cells are lined up and hit with a laser where the emitted light gives information on cell size, granularity and fluorescence.</i>	8
2.3	<i>Fluorescence-activated cell sorting. The cells are divided into individual droplets after being hit by the laser beam. Based on the emission, a charge can be applied to the drop which enables sorting using a static electrical field.</i>	9
2.4	<i>Example of a dot plot with CFSE and Live/Dead staining. Four cell populations can be identified. The target cells are identified using the high CFSE signal on the x-axis and the dead cells can be recognized by the high Live/Dead signal on the y-axis.</i>	10
2.5	<i>The function of the T7 Endonuclease I assay. Wild-type DNA and mutant DNA are denatured and hybridized. The created mismatch is recognized by the T7EI enzyme which creates the cleaved fragments that are visualized on a gel.</i>	12
3.1	<i>Separation between the different layers in a buffy coat before and after density gradient centrifugation.</i>	14
3.2	<i>An example of gating strategies for cytotoxicity assay using CFSE and Live/Dead stain.</i>	15
4.1	<i>Specific lysis of K562 cells with primary NK cells (n=3, error bars represent SEM). Blocking antibodies were used to block individual receptors on NK cells to study its effect on target cell lysis.</i>	24
4.2	<i>Amplification plots from RT-qPCR for genes a) PVR, b) NECTIN2, c) MICA/MICB, d) ULBP1, e) ULBP2 and f) ULBP3. K562 cells are shown in dark green and 721.221 cells are shown in light green.</i>	25

4.3	<i>Amplification plots from RT-qPCR for genes a) CD48, b) CD58, c) NCR3LG1, d) CLEC2B and e) BAG6. K562 cells are shown in dark green and 721.221 cells are shown in light green.</i>	25
4.4	<i>Experiment for determining the optimal blasticidin concentration for selection of transduced K562 cells. The images display the dot plots for cells cultured with 20µl/ml (left) and 30µl/ml (right) blasticidin respectively. The live cells are gated.</i>	26
4.5	<i>Results from Western blot for verification of Cas9 expression in six clones. As negative control, wild-type K562 was used.</i>	28
4.6	<i>Insert for gRNA in form of gblock. The design include from left to right: 6 bp from end for RE, recognition site for RE XhoI, stop codon for FP, short spacer, poly A tail, spacer, U6 promoter, recognition sites for RE BbsI, gRNA scaffold, recognition site for RE BamHI and 6 bp from end for RE.</i>	29
4.7	<i>crRNA for the gene NCR3LG1 with overhangs for RE BbsI digestion.</i>	30
4.8	<i>Cell viability and transfection efficiency results from K562 transfection with mEGFP-C1+NCR3LG1 gRNA3 plasmid 48h post transfection.</i>	30
4.9	<i>Cell viability and transfection efficiency results from K562 transfection with EBFP2-C1+PVR gRNA3 plasmid 48 h post transfection.</i>	31
4.10	<i>Cell viability and transfection efficiency results from K562 transfection with mEGFP-C1+NCR3LG1 gRNA3 and EBFP2-C1+PVR gRNA3 plasmids 72 h post transfection.</i>	31
4.11	<i>Result from T7EI assay, performed 6 days post transfection with gRNAs for NCR3LG1 and PVR genes. The visible fragments verifies Cas9 functionality.</i>	32
4.12	<i>Gel electrophoresis result from T7EI assay, performed 6 days after transfection with gRNAs for NCR3LG1 and PVR genes.</i>	33
4.13	<i>Histograms showing Alexa Fluor 488 intensity from staining of B7-H6 in gRNA-transfected K562 cells. Left histograms (A-H) show the pooled clones from all rows. Middle histograms show the single clones from row B and the right histograms show four clones from row H. The negative and the positive controls are displayed as grey peaks in all histograms and the samples are displayed as a black peak.</i>	34
4.14	<i>Histograms showing Alexa Fluor 488 intensity from staining of PVR in gRNA-transfected K562 cells. Left histograms (A-H) show the pooled clones from all rows. Middle histograms show the single clones from row A and right histograms show four clones from row D. The negative and the positive controls are displayed as grey peaks in all histograms and the samples are displayed as a black peak.</i>	35

-
- 4.15 *Histograms showing Alexa Fluor 488 intensity from staining of B7-H6 and PVR in doubly gRNA-transfected K562 cells. Histograms (A-H) show the pooled clones from all rows. The left histograms show the B7-H6 stained pooled clones and the right histograms show the same clones, stained for PVR. The negative and the positive controls are displayed as grey peaks in all histograms and the samples are displayed as a black peak. 36*
- 4.16 *Histograms showing Alexa Fluor 488 intensity from staining of B7-H6 and PVR in doubly gRNA-transfected K562 cells. Histograms (A-H) show the single clones from row C. The left histograms show the B7-H6 stained clones and the right histograms show the same clones, stained for PVR. The negative and the positive controls are displayed as grey peaks in all histograms and the samples are displayed as a black peak. 37*

List of Tables

3.1	<i>Ligand expression studied with RT-qPCR and the corresponding NK cell receptor.</i>	16
3.2	<i>Experiments for testing of optimal blasticidin concentration for selection.</i>	17
3.3	<i>crRNA sequences for the genes NCR3LG1, PVR and NECTIN2.</i>	19
3.4	<i>Plasmids used in the current project. All were obtained from Addgene, deposited by Michael Davidsons lab.</i>	20
3.5	<i>Parameters for Neon transfection system used for transfection of K562 cell line.</i>	21
4.1	<i>Gene expression of ligands in K562 and 721.221 cells, studied by RT-qPCR. The symbol \checkmark indicates expression.</i>	26
4.2	<i>Median fluorescence intensity values of BV421 for Cas9 expression in six clones with unstained control, secondary antibody control and K562 wild-type control.</i>	27
4.3	<i>Median fluorescence intensity values of BV421 in Cas9 primary antibody titration using clone 10A11 and K562 wild-type. Unstained control and secondary antibody control were included.</i>	27
4.4	<i>Result from transfection of K562, obtained using flow cytometry 48 h and 72 h post transfection.</i>	31
A.1	<i>Primers used for RT-qPCR.</i>	I
A.2	<i>PCR primers used for T7 Endonuclease I assay.</i>	I
A.3	<i>crRNA oligomers. The underlining show the complementary part.</i>	II
B.1	<i>Program for reverse transcription.</i>	III
B.2	<i>Program for qPCR.</i>	III
B.3	<i>PCR program for T7EI.</i>	V

List of Abbreviations

ADCC	Antibody-dependent cell cytotoxicity
APCs	Antigen-presenting cells
BCR	B cell receptor
BSA	Bovine Serum Albumin
cDNA	Complementary DNA
CML	Chronic myeloid leukemia
Cq	Cycle quantification
CRISPR	Clustered Interspaced Short Palindromic Repeats
DMEM	Dulbecco's Modified Eagle Medium
dsDNA	Double stranded DNA
FACS	Fluorescence-activated cell sorting
FP	Fluorescent proteins
FSC	Forward-scattered light
HRP	horseradish peroxidase
IL-2	Interleukin 2
IMDM	Iscove's Modified Dulbecco's Medium
ITIM	Immunoreceptor tyrosine-based inhibitory motif
KIRs	Killer-cell immunoglobulin-like receptors
MCS	Multiple cloning site
MHC	Major histocompatibility complex
NCRs	Natural cytotoxicity receptors
NHEJ	Non-homologous end joining
NK	Natural Killer cell
NRT	No reverse transcriptase
NTC	No template control
PAM	Protospacer adjacent motif
PAMP	Pathogen associated molecular patterns
PBMC	Peripheral blood mononuclear cell
PEST	Penicillin/streptomycin
PRR	Pattern recognition receptors
RE	Restriction enzyme
RT-qPCR	Real time quantitative PCR
SSC	Side-scattered light
T7EI	T7 Endonuclease I
TCR	T cell receptor

1

Introduction

Cancer is one of the leading causes of morbidity and mortality globally with 14,1 million new cases in 2012 and 8,8 million deaths from the disease in 2015 [1, 2]. As the population increases in combination with aging, the burden is expected to grow. The statistics show that the already considerable economic burden of cancer is increasing and in 2010 the annual cost was estimated to US\$ 1.16 trillion [1, 2]. Cancer immunotherapy attempts to make use of the specificity of the immune system to treat disease and it can be used as an alternative to radiation, chemotherapeutic agents and surgery-based cancer treatments [3]. It has shown successful in many different forms of cancer, such as malignant melanoma, lung cancer and renal cell cancer.

Among all, natural killer (NK) cells have been shown to be important in host immunity towards cancer [4]. NK cells are important cells in the innate immune system and are considered to be vital in fighting cancer and virus infection as well as regulating the immune response. During the last two decades, the knowledge of NK cells has increased and contributed to important insights in their function and purpose in normal immune responses [5]. An increased knowledge in NK cell recognition mechanisms could potentially contribute to new advances in immunotherapy and for characterizing tumour types [6].

1.1 Aim

The long-term aim of this project was to define ligand candidates for the activating receptor, NKp46, of NK cells. The intermediate aims included:

- Defining receptors involved in NK cell cytotoxicity of K562 cell line
- Generating a Cas9-expressing K562 cell line
- Designing and generating gRNAs for knockout of ligands involved in NK cell cytotoxicity of the K562 cell line
- Creating a K562 cell line with selected ligand genes knocked out and determining how the altered ligand repertoire affects susceptibility to NK cell cytotoxicity

Finally, the ultimate goal comprised transfection with a gRNA library to obtain stochastic deletion of genes and using new generation sequencing and bioinformatics, acquiring candidate genes for the NKp46 receptor ligand.

1.2 Clarification of the issue under investigation

The first part of the project was designed to study the dependence on the different activating receptors on NK cells in regard to killing of NK cell-sensitive cells. RT-qPCR analysis was also performed to study the gene expression of ligands for the activating receptors. In parallel, a K562 cell line expressing Cas9 was generated using a lentiviral vector. The engineered cell line was used to knock out genes encoding ligands for key activating receptors, with the aim to create a cell line that is killed in a more NKp46-dependent way. gRNAs for the target genes were designed and plasmids containing these, were constructed. The plasmids were used to transfect the Cas9-expressing monoclonal cell line to enable the gRNA-Cas9 complex to knock out the ligand genes. The transfection was verified using flow cytometry and the cleavage was confirmed using a T7EI assay. A reduced expression of the proteins was also verified using flow cytometry.

Due to the magnitude of the project, the final parts will be pursued in future studies. The plan is described below for full understanding of the project as a whole.

The knockout of the key ligands reduce the importance of the corresponding NK cell receptors in K562 cell elimination. The gradual shift in significance of the individual receptors will be monitored and the K562 cell sensitivity towards NK cells is hypothesized to decrease overall, but with an increase in NKp46 dependence. The decreased sensitivity may require higher effector/target ratio for an efficient target killing.

The ultimate goal is to expose the generated cell line to a genome-wide library of gRNAs to create stochastic deletion of genes. The acquired cell line will then be exposed to NK cells which will favour the cells with mutations that decreases their susceptibility to NK cell cytotoxicity. Among the surviving cells, there will be a relative abundance of cells with deletions in genes encoding NK ligands, as compared to control cells exposed to medium alone. Next-generation sequencing can be used to compare control cells to the NK cell-exposed cells and through bioinformatics, candidate genes for the NKp46 ligand can be acquired.

2

Theory

The current section presents theory regarding the immune system with focus on one specific immune cell; the natural killer cell. Background to the used cell lines and methods such as flow cytometry, cytotoxicity assay, RT-qPCR and CRISPR/Cas9 will also be explained.

2.1 The immune system

The basic function of the immune system is to protect the body from infectious microbes. The mammalian immune system is generally divided in two types of defences; the innate and the adaptive immune system [7, 8]. The innate immune system is composed of a variety of protective mechanisms that include anatomical barriers and a variety of myeloid and lymphoid cells. The adaptive immune system, instead relies mainly on the two lymphocytes B- and T cells. By expressing a large repertoire of antigen receptors, generated by recombined gene segments, these cells can combined recognize most pathogens and as a response, produce antibodies and cytokines as well as exert cytotoxic functions [8].

2.1.1 Innate immune system

The protective layer that shields the inside of the body from the outside world is generally considered to belong to the innate immune system [7]. The layer is made up of a barrier of epithelial surfaces that include the skin and linings for respiratory, intestinal and urinary tracts. A layer of mucus covering internal epithelial surfaces creates additional protection as it inhibits microorganisms to physically adhere to the surfaces. This is further supplemented by the movement of the cilia on the epithelial cells that also aid in clearance of the pathogens. The mucus also contains substances that have the ability to kill pathogens or at least inhibit their proliferation [7].

If pathogens manage to penetrate the physical and chemical barriers, pathogen-exposed cells also have an ability to sense an intruder. A major function of the infected cell is the ability to recognize and degrade double stranded RNA since it is a common intermediate in viral replication [7]. The cell can also commit suicide by initiating apoptosis if infected [7].

The next line of innate immune defense constitutes the specialized cells and proteins that by recognizing conserved parts of pathogens, can initiate a fast response and kill the microorganism. Professional phagocytic cells such as macrophages and

neutrophils as well as natural killer cells and the complement system comprise this defense [7]. The innate immune response is not specific to a certain pathogen in the same way as the adaptive response is. The cells of the innate immune system have several different receptors that are inherited through the germline and developed to recognize chemical groups, present in molecules associated with microbes [9]. The chemical groups are often connected to important conserved functions and can be present in several microorganisms but are not found in mammals. The molecules are called *pathogen associated molecular patterns* (PAMP) and the correlating receptors *pattern recognition receptors* (PRR) [9, 10].

2.1.2 Adaptive immune system

The second part is the adaptive immune system. As the name indicates, it has an ability to adapt to the infection and its two main attributions are the specificity caused by the recombination of the receptor genes and the ability to remember specific microbes and cause a stronger response upon re-infection, called memory [9]. The two main players of the adaptive immunity are the two lymphocytes B- and T cells. B cells have the ability, upon activation by cell surface-bound or soluble antigens, to differentiate into antibody-secreting plasma cells. Instead, T cells recognize foreign peptides bound to endogenous proteins called *major histocompatibility complex* (MHC) that are expressed by other cells [11]. This cause T cell activation, which results in different actions depending on subpopulation of T cell. The two major subsets are $CD8^+$ cytotoxic T cells that upon activation act to eliminate the infected cells or the $CD4^+$ helper T cells that stimulate other cells by secretion of cytokines[12].

The receptors of both lymphocytes are created by recombination of one gene during cell development [10]. Each cell is then divided, where each daughter cell inherits the same combined receptor gene resulting in expression of the same receptor. Due to this recombination of the receptor gene, there are many different B- and T-cell receptors (BCR and TCR respectively) in the body but few cells within the same clone. Upon recognition of an antigen, the activated cell starts to expand to create more cells within the clone, with the same receptor that can recognize the specific antigen for the infection. The process is called clonal expansion and describes the adaptiveness of the response [9].

Antigen-presenting cells (APCs), such as dendritic cells and macrophages, are innate immune cells that act as bridges between innate and adaptive immunity. These cells process and present antigen-peptides bound to the MHC molecules to the antigen-specific TCR in order to activate T cells [12]. The antigen-peptides originate from proteins taken up by APCs through an endocytic process. Following fragmentation of these proteins, the peptides are loaded into the MHC complex to be expressed on the surface. $CD4^+$ T cells with TCRs capable of recognizing the peptide can then bind MHC class II complex to be activated, while $CD8^+$ bind MHC class I [12, 13]. Despite the seemingly strict division between the two types of immune responses, the constant interaction between them in the form of antigen presentation and cytokine secretion as well as formation of memory-like innate immune cells, erases the lines separating them and creates the image of a highly complex system [12].

2.2 Natural Killer Cells

The NK cell was discovered in 1975 and is considered to be important in the early innate immune responses [8, 11, 13]. The effector functions of NK cells include elimination of transformed and infected cells without prior sensitization as well as secretion of cytokines and chemokines that regulate the immune response [11, 14]. NK cells are defined as $CD3^-CD56^+$ lymphocytes with $CD56^{bright}$ and $CD56^{dim}$ subsets [15]. The largest part of NK cells present in peripheral blood and the spleen are identified as $CD56^{dim}CD16^+$ cells and have higher cytotoxic capacity toward target cells. NK cells present in tonsils and lymph nodes are on the other hand identified as $CD56^{bright}CD16^-$ subset and have historically been ascribed immunoregulatory functions by secretion of cytokines [11]. More and more data identify this subset as a progenitor subset to the more differentiated $CD56^{dim}$ NK cells [11, 14].

NK cells can often be confused with T cells and the two cell types have many parts in common such as similar morphology, function, as well as expression of several surface molecules. NK cells are however generally considered to belong to the innate immune system since NK cell receptors are encoded from intact genes, inherited through the germline, in contrast to the receptors in the adaptive immune system that are generated from recombined gene segments [16, 11].

2.2.1 The "missing self" theory

The "missing self" theory was presented in 1981 by Klas Kärre [17] since cells lacking MHC class I were shown to be targeted by NK cells, which are educated during maturation to be able to recognize absence of "self". MHC class I is present on all normal cells but can be downregulated in cancer cells or virally infected cells [11]. The "missing self" theory explains how NK cells can intercept transformed or infected cells that successfully avoid the detection of T cells. Figure 2.1 explains the difference between T cells and NK cells in recognition of target cells. It is shown that, in contrast to T cells that discriminate between self and foreign peptides bound to the MHC class I complex, NK cells recognize the MHC complex itself where a lack of the molecule contributes to elimination of the target. As displayed in Figure 2.1, pathogens, for example herpes viruses can try to escape the immune system by preventing the normal expression of MHC class I. Also tumorigenesis can lead to mutations in genes vital for the MHC processing machinery and change the expression of MHC molecules. These mechanisms can lead to evasion of T cell detection but the lack of the molecule will put the cells in higher risk for detection by NK cells [13]. The "missing self" hypothesis did not, however, account for the cases where absence of MHC class I did not result in killing of the target cell. The discovery of activating and inhibitory receptors led to further development of the understanding of the complex signalling between different receptors that helps NK cells distinguishing between normal and unhealthy cells [8, 13].

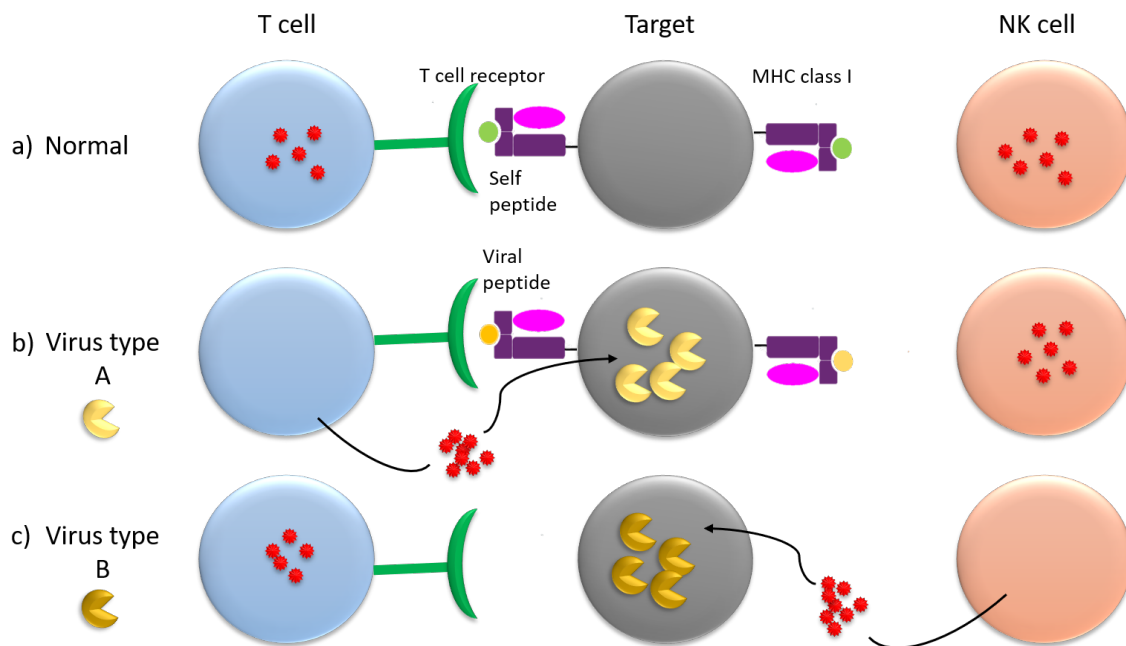


Figure 2.1: *Difference in recognition mechanism between T cells and NK cells. a) Normal cells expressing MHC class I molecules with bound self-peptides are resistant to both lymphocytes. T cells recognize the MHC class I molecule that presents viral peptides, b), but fail to detect infected cells with downregulated MHC class I c). Instead NK cells do not generally discriminate between self and viral peptides but rather the expression of MHC class I itself, which is shown in b) and c). Virus B evades T cell detection due to downregulation of MHC class I, which is instead recognized by the NK cell, resulting in target cell lysis.*

2.2.2 Inhibitory NK cell receptors

Inhibitory receptors include the inhibitory killer-cell immunoglobulin-like receptors (KIRs) and NKG2A that bind the MHC class I molecules expressed by normal cells. The inhibitory KIRs (iKIRs) and NKG2A have intracytoplasmic tails containing pairs of immunoreceptor tyrosine-based inhibitory motifs (ITIMs) that transduce the inhibitory signal [18]. These receptors inhibit NK cell activation and killing of the target cell which is a crucial function in order to protect healthy cells [13]. The inhibitory receptors have also been discovered to have a second function which instead paradoxically helps in making the cells more responsive to activation. Studies have shown that NK cells acquire their functional competency by engagement between its inhibiting receptors and the host MHC class I molecules in a process called licensing or education. NK cells lacking inhibitory receptors that recognize self-MHC class I molecules will remain unlicensed/uneducated and therefore hyporesponsive [19, 20].

2.2.3 Activating NK cell receptors

There are also several activating receptors that can either interact with soluble ligands or with membrane-bound ligands on target cells. An important function of the NK cell activating receptors is their ability to detect self-molecules that are upregulated upon cellular stress [6]. NK cells can also target antibody-coated cells using its cell surface receptor CD16 that can detect the Fc-region on IgG antibodies and thereafter exert antibody-dependent cell cytotoxicity (ADCC) [10]. Important activating receptors include NKG2D, DNAM-1, 2B4 and the natural cytotoxicity receptors (NCRs) NKp46, NKp30 and NKp44 [8]. Ligands for NKG2D (MICA/MICB and ULBP1-3), DNAM-1 (PVR and NECTIN2), 2B4 (CD48), NKp30 (B7-H6 and BAG6) and NKp44 (MLL5) have previously been discovered but there is still no endogenous ligand known for the activating receptor NKp46 [21, 22, 6].

Upon activation, NK cells exert their cytotoxic function, which is similar to CD8⁺ T cells. Both cell types contain granules with proteins that can induce killing of the target. When activated, the cells release the content of the granules adjacent to the target cells. The protein called perforin enables entry of other proteins called granzymes that can initiate killing of the cell [11].

2.3 Cell lines

Much of what is known about NK cells, has been discovered using cytotoxicity experiments, described more in detail in Section 2.5. MHC class I-deficient cells have frequently been used since their lack of MHC- I expression makes them incapable of generating inhibitory signals in NK cells, which makes it possible to only study the activation mechanism [23]. Two examples of these cells are the K562 and 722.221 cell lines that have been used in the current project. The K562 cell line is derived from a patient suffering from chronic myeloid leukemia (CML) in blast crisis and 722.221 is a human B-lymphoblastoid cell line [24, 25].

2.4 Flow cytometry

Flow cytometry is a powerful tool that measures fluorescence and light scatter from individual cells which can give information on cell size, density and specific cellular constituents [26]. As can be seen in Figure 2.2, single cells in an injected cell suspension are directed through a laser beam in sheath fluid. Once hitting the cell, the excitation light creates both forward (FSC) and side scatter (SSC) of which the first indicates the size of the cell and the latter gives indication of the granularity of the cell. This can be combined with fluorescent-labeled antibodies to specific proteins and surface markers on the cells to distinguish cell populations [27]. Fluorescent proteins such as GFP and BFP that are expressed by certain cells can also be detected. The lasers present in the flow cytometer affects what fluorophores and fluorescent proteins that can be detected since all fluorescent molecules have different excitation spectra [27, 26]. Exposure to a laser beam at the correct excitation

wavelength will cause the fluorescent molecule to absorb the energy and emit it at a longer wavelength due to loss of energy, referred to as Stoke's shift [28]. The emitted light is guided through different filters and detected by sensitive detectors that convert the light pulses to electrical pulses that are digitized by the electronic system. Specialized software can then present the data graphically [27, 26].

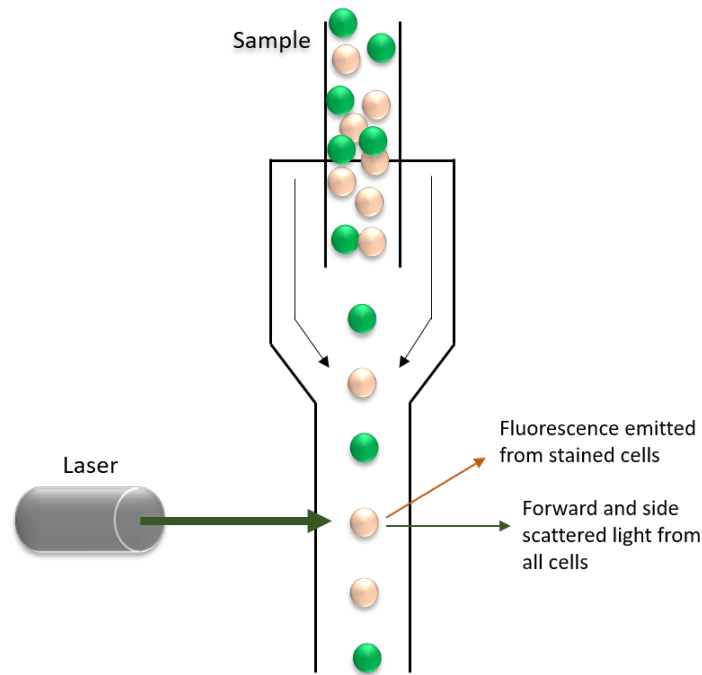


Figure 2.2: *Flow cytometry schematic. Cells are lined up and hit with a laser where the emitted light gives information on cell size, granularity and fluorescence.*

Fluorescence-activated cell sorting (FACS) utilizes the principle of flow cytometry to separate cells with specific light-scattering or fluorescent characteristics. As seen in Figure 2.3, the injected cell suspension is lined up in the stream which is broken up into individual droplets by a vibration mechanism directly after passing through the laser beam. A signal pulse is generated based on the light emission caused by the cell passing the laser beam. If the amplitude of the signal pulse is within predetermined limits, a charge will be applied to the droplet. The drop then passes through a static electrical field that divert it based on its charge, making it possible to collect cells of interest [29, 30].

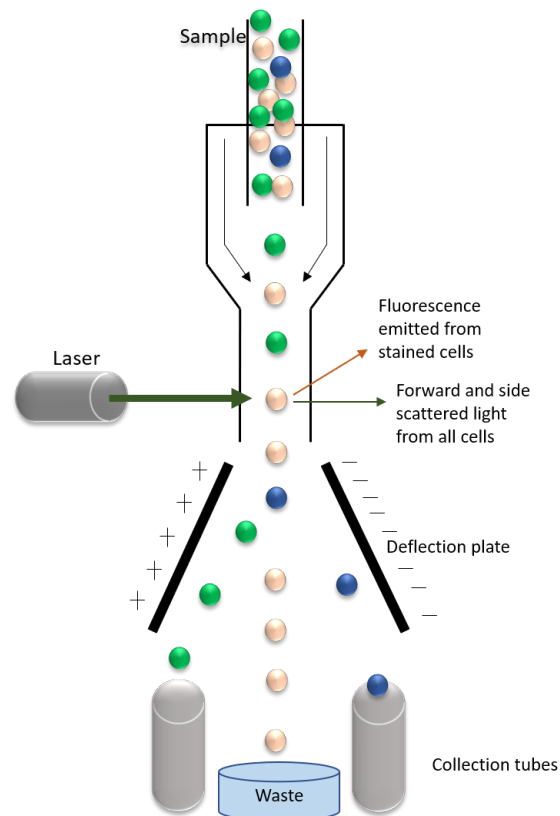


Figure 2.3: *Fluorescence-activated cell sorting. The cells are divided into individual droplets after being hit by the laser beam. Based on the emission, a charge can be applied to the drop which enables sorting using a static electrical field.*

2.5 Cytotoxicity Assay

Cytotoxicity assays are used to measure NK cell activity against different target cells. The chromium-51 (^{51}Cr) release assay is considered the "gold standard" for measuring NK cell and cytolytic T cell cytotoxicity and it involves labelling of the target cells using ^{51}Cr , which enters the cells and binds to intracellular proteins [23]. Upon co-incubation together with the effector cells (NK cells), the specific NK cell activity can be determined by measuring the amount of released ^{51}Cr into the culture medium [23, 31]. Due to the health hazard ^{51}Cr imposes, combined with a limit in the number of different analysis possible, flow cytometry assays have been developed as a substitute. The general principle is to stain the target cells with a primary fluorochrome to enable discrimination between target and effector cells. This could for example be 5-(6)-Carboxy-fluorescein succinimidyl ester (CFSE). The addition of a secondary fluorochrome, that either binds DNA in cells with disrupted membranes or interact with amines, mostly present inside the cell, help distinguish dead cells after co-culture at different effector target (E:T) ratios [23]. An example of a dot plot from a cytotoxicity experiment with CFSE and Live/Dead stain is visible in Figure 2.4. Four different populations can be distinguished. The cells with high CFSE signal are the target cells and of these, the cells with a high live/dead signal are dead. The cells with a low CFSE signal are the effector cells and again,

the cells with a high signal for live/dead are dead. Other antibodies that could be of interest to use in a cytotoxicity assay are antibodies that bind CD107 and IgM antibodies specific for certain NK cell receptors. The antibody to CD107 can be used to monitor the degranulation of NK cells since it binds the lysosomal-associated membrane protein-1 (LAMP-1 or CD107a) that lines the membrane of the intracellular cytolytic granules in the NK cells [32]. During degranulation, the content of the cytolytic granules is emptied and the CD107 instead appears on the outside of the NK cell membrane [32]. The IgM antibodies block the receptors they bind to and prevent these from involvement in killing of the target cells. The use of IgM also avoids ADCC which would be a risk with the use of IgG.

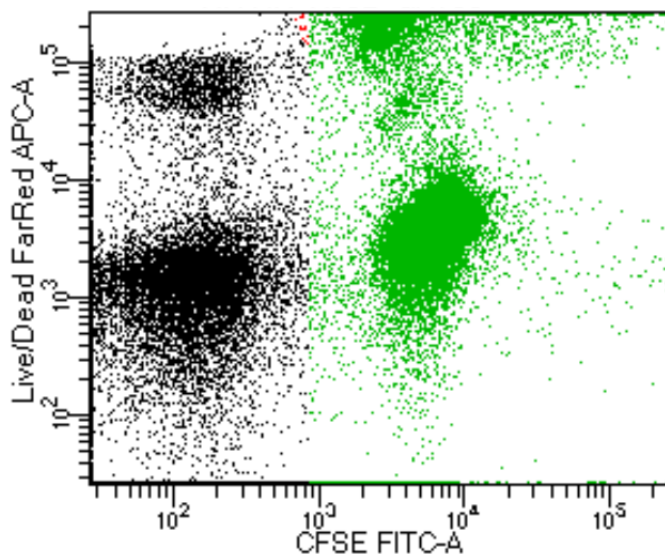


Figure 2.4: *Example of a dot plot with CFSE and Live/Dead staining. Four cell populations can be identified. The target cells are identified using the high CFSE signal on the x-axis and the dead cells can be recognized by the high Live/Dead signal on the y-axis.*

2.6 RT-qPCR

Real time quantitative PCR (RT-qPCR) is a quick and sensitive method for detection and quantification of RNA. The method involves a reverse transcription (RT) procedure followed by a qPCR step. In the RT step, RNA is converted into complementary DNA (cDNA) by the use of the enzyme reverse transcriptase. The second part involves using the cDNA as template during the qPCR step. Fluorescent reporter molecules that bind DNA are used to enable measurement of the amplification of the DNA in each cycle [33, 34].

2.7 CRISPR/Cas9

CRISPR (Clustered Interspaced Short Palindromic Repeats)/Cas9 (CRISPR associated protein 9) is a bacterial defence system that has been discovered to be a huge asset in genome engineering. The engineered CRISPR system contains the two components; Cas9 endonuclease and a guide RNA (gRNA). The gRNA is a short synthetic RNA composed of a scaffold sequence, also called tracrRNA needed for Cas9 binding and a ~ 20 bp short spacer sequence, also named crRNA, that is specific for the targeted gene. The gRNA has to be unique compared to the rest of the genome and localized close to a protospacer adjacent motif (PAM). The PAM sequence is important for target binding and is different depending on what strain the Cas9 protein originates from. For *Streptococcus pyogenes* Cas9, the PAM sequence is 5' NGG 3' [35].

The two components, Cas9 and the gRNA, form a complex and if sufficient homology between the spacer and the target DNA exist, the Cas9 enzyme will create a double stranded break. This can be repaired by the cell in two ways: the less efficient but high fidelity homology directed repair or the efficient but also more error-prone non-homologous end joining (NHEJ) [7]. NHEJ is the most active repair mechanism and it frequently creates nucleotide insertions or deletions at the repair site. The unpredictability of NHEJ leads to random mutations in a population expressing Cas9 and a gRNA. NHEJ will in most cases result in amino acid insertions, deletions or frameshift mutations leading to premature stop codons with the ideal result being a loss of function mutation within the targeted gene [35].

2.8 T7 Endonuclease I Assay

The T7 endonuclease I (T7EI) assay is a tool used to enable detection of mutations created using for example CRISPR/Cas9 ???. The mutation detection assay utilizes heteroduplex DNA from denatured and hybridized mutant and wild-type DNA, as seen in Figure 2.5. The enzyme T7EI has the ability to recognize and cleave double stranded DNA (dsDNA) at mismatches created by single or several nucleotides. The resulting cleaved fragments can then be visualized using gel electrophoresis [36, 37].

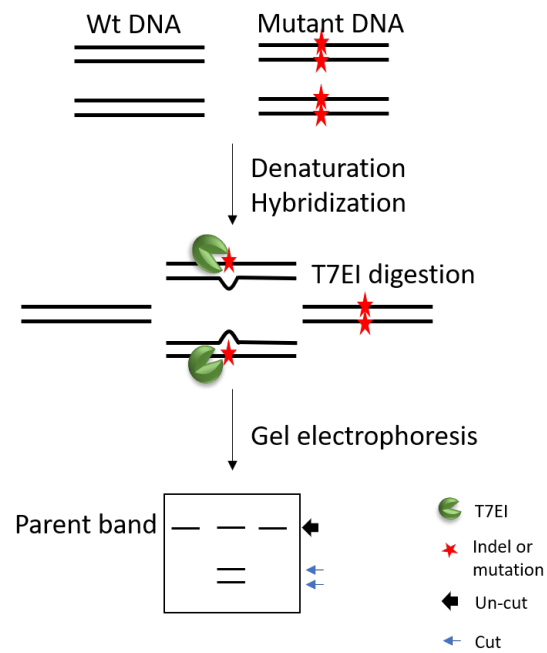


Figure 2.5: *The function of the T7 Endonuclease I assay. Wild-type DNA and mutant DNA are denatured and hybridized. The created mismatch is recognized by the T7EI enzyme which creates the cleaved fragments that are visualized on a gel.*

3

Methods

3.1 Culture conditions

All cells were cultured at 37°C in a humidified 5% CO₂ incubator. The medium used for K562 cell line was based on Iscove's Modified Dulbecco's Medium (IMDM) (Thermo Fisher Scientific) with 10% heat inactivated (HI) fetal calf serum (FCS), 1% sodium pyruvate and 1% L-Glutamine, along with 1% penicillin/streptomycin (PEST). The cells were split approximately 1:5 every second day.

Single cell culture of K562 cells was performed using the same IMDM complete medium with 1% PEST with medium change when needed based on the colour change.

During viral transduction the medium used was based on Dulbecco's Modified Eagle Medium (DMEM) (Sigma-Aldrich) with addition of 10% HI FCS and 2% L-Glutamine and supplemented with 30 µg/ml blasticidin during selection.

For electroporation of K562 cells, the IMDM complete medium was used without PEST immediately after transfection but it was added to medium after 6 days.

For freezing of cells, 0,5-1 ml Cell Culture Freezing Media (Thermo Fisher Scientific) containing 10% DMSO and FCS was used.

For 721.221 cell line, the culture medium was based on RPMI with 10% HI FCS and 1% L-Glutamine, along with 1% PEST.

3.2 Cell separation and NK cell cytotoxicity

Primary NK cells were isolated and purified from day-old buffy coats obtained from Sahlgrenska blodcentral (Blood center). For separation of PBMC (PBMC), one buffy coat of approximately 10 ml was mixed with 15 ml room tempered buffered NaCl (buNaCl) in a 50 ml Falcon tube. 25 ml room tempered 2% dextran was added to increase erythrocyte aggregation, the tube was inverted carefully and left on bench to sediment for 20 min or until there had appeared a clear line between the two layers. Two new 50 ml Falcon tubes had been prepared with 15 ml room tempered lymphoprep (STEMCELL Technologies) with added NaCl to which the top layer of sedimented buffy coat was distributed carefully in order to maintain the separation between the two. The two Falcon tubes were centrifuged at 850xg for 20 min at 20°C. After the density gradient centrifugation, different layers had formed, visible in schematic Figure 3.1. PBMC was identified as a thin, cloudy white layer in the middle of the tube whereas erythrocytes and granulocytes had formed a pellet at the bottom of the tube. The PBMC layer was transferred to a new Falcon tube.

3. Methods

The PBMC was then washed with cold elution buffer (PBS supplemented with 0.5% BSA and 2 mM EDTA) twice by centrifugation at 350xg for 7 min, at 4°C (standard settings) and placed on ice before cells were resuspended in approximately 10 ml cold elution buffer and counted using a Z2 coulter counter (Beckman Coulter). For counting, 20 µl cell suspension was transferred to a plastic cuvette, followed by addition of 10 ml isoton solution and counted. Antibodies to CD3 and CD56 were used to analyze percentage of NK cells in PBMC in Accuri C6 flow cytometer (BD Biosciences). Based on the cell concentration, the NK cell percentage in PBMC and the amount of NK cells wanted, the volume PBMC suspension needed was calculated with margins for losses during isolation.

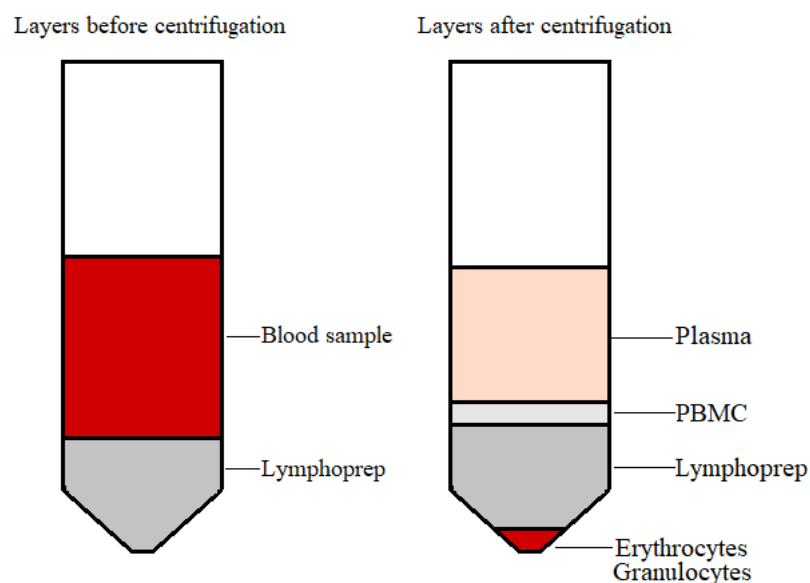


Figure 3.1: *Separation between the different layers in a buffy coat before and after density gradient centrifugation.*

For NK cell isolation, MACS isolation kit (Mitenyi biotec) was used. The calculated volume PBMC was washed using standard settings and the cells were resuspended in 40 µl elution buffer per 10^7 PBMC cells. 10 µl of NK Cell Biotin-Antibody cocktail per 10^7 PBMC cells was added and mixed well, followed by incubation in fridge for 5 min. 30 µl elution buffer per 10^7 cells was added to the tube, followed by 20 µl NK Cell Microbead Cocktail per 10^7 PBMC cells. The suspension was mixed well and incubated for 10 min in fridge. The sample was then diluted to a volume of at least 500 µl with elution buffer. A LS column was placed in the magnetic field on the MACS separator and prepared. A 10 ml tube was placed under the column and the cell suspension was added, followed by 3 x 3 ml elution buffer to elute the cells from the column. 50 µl of the NK cell suspension was again incubated with CD3/CD56 antibody (1:100) for 20 min in room temperature to study the purity of the sample using Accuri C6 flow cytometer (BD Biosciences). The cell suspension was centrifuged with standard settings and resuspended in 1 ml RPMI

medium supplemented with 10% FCS and 1% PEST and counted. The NK cells were incubated at 37°C in 96-well plate, with 200 000 cells/well, overnight or over weekend in complete RPMI media, with or without supplementary stimulation of 100 u/ml interleukin 2 (IL-2).

K562 cells were washed in buNaCl and stained with CFSE (1:700)(Invitrogen). 50 000 K562 cells and varying numbers of NK cells were incubated in 96-well plate with effector/target ratios 1:1 and 2:1 for 4h at 37°C. Different antibodies were also incubated with the cells depending on experiment. Antibodies to LAMP-1/CD107 (CD107a-PE-Cy7, BD Pharmingen) were used to study degranulation of NK cells and a variety of blocking antibodies (Moretta lab) were used to block receptors on NK cell membrane to study their individual significance on NK cell lysis of target cells. These receptors included NKp46 (clone KL247), NKp30 (clone F252), NKp44 (clone KS38), DNAM-1 (clone F5), 2B4 (clone Co54), CD2 (clone QA196) and NKG2D (BAT221, Miltenyi Biotech). After 4 hours, the cells were stained with FarVid (Invitrogen) (1:1000) and analyzed to study target cell lysis in a five-laser BD LSRFortessa flow cytometer (405, 488, 532, 640 nm and UV lasers, BD Biosciences). A gating example is given in Figure 3.2.

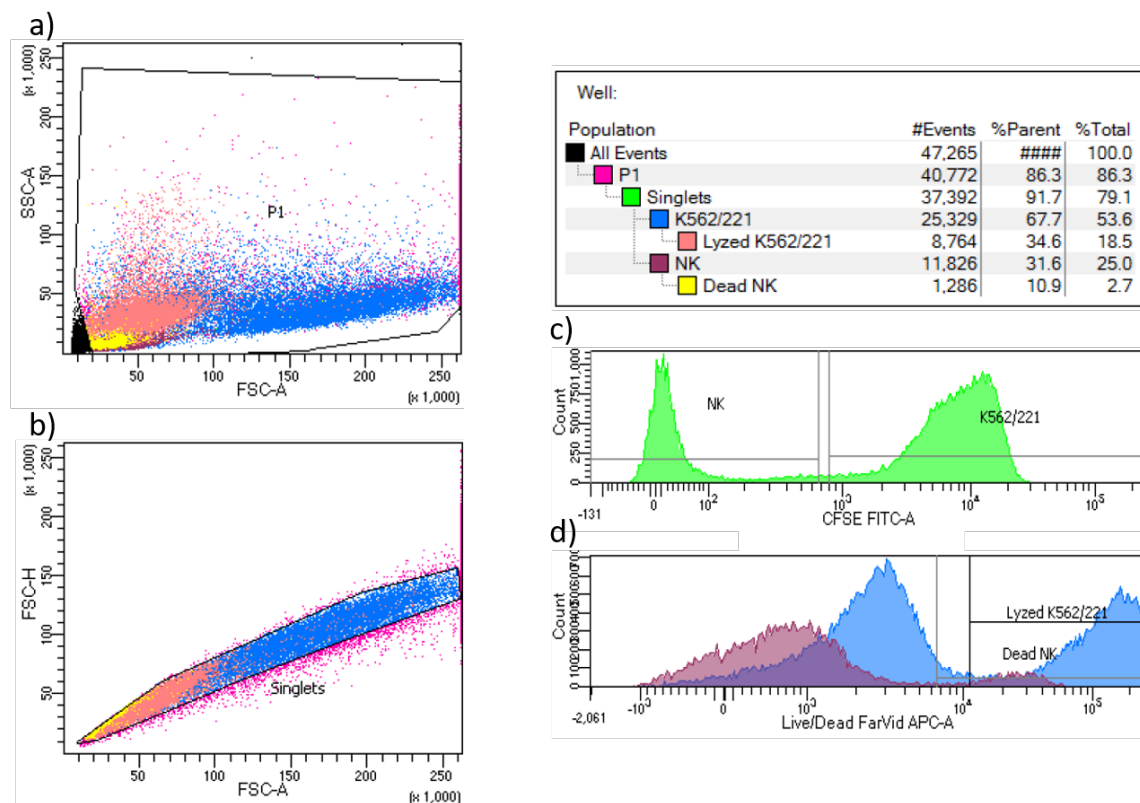


Figure 3.2: An example of gating strategies for cytotoxicity assay using CFSE and Live/Dead stain.

Figure 3.2 show the gate in dot plot a) that is based on FSC and SSC, that give information on size and intracellular complexity, to remove debris and to ensure that only cells are studied in the next plot. The following gate in dot plot b) is used to gate in single cells and remove doublets. The gate in histogram c) is based on the

intensity of the CFSE that was used to stain K562 cells in order to separate them from NK cells. The gate in histogram d) use the intensity of the Live/Dead stain to discriminate between live and dead cells.

Specific lysis was calculated using Equation 3.1.

$$\frac{\% \text{ lysis for each experimental condition} - \% \text{ lysis in control condition}}{100 - \% \text{ lysis in control condition}} \quad (3.1)$$

3.3 RT-qPCR

RT-qPCR was used to study the gene expression of several NK activating receptor ligands in K562 and 721.221 cells. 721.221 cells were included in this experiment since it also is a leukemic cell line and it would be interesting to compare the two. Table 3.1 presents the ligands studied and the corresponding NK cell receptor.

Table 3.1: *Ligand expression studied with RT-qPCR and the corresponding NK cell receptor.*

Ligand	Corresponding receptor
PVR	DNAM-1
NECTIN2	DNAM-1
MICA/MICB	NKG2D
ULBP1-3	NKG2D
CD48	2B4
CD58	CD2
B7-H6	NKp30
BAG6	NKp30
CLEC2B	NKp80

A PCR plate was prepared with 5 μ l Bovine Serum Albumin (BSA) (Thermo Fisher Scientific, BSA 20 mg/ml, 5mg #B14), diluted 20x in RNase free water and 100 K562 and 721.221 cells were sorted in 4 wells each using a BD FACS ARIA. The cells were frozen at -80°C to lyse. Reverse transcription reaction mixture was prepared, using the 5 μ l RNA to a 10 μ l reaction with TATAA GrandScript RT Reaction Mix (5x) and TATAA Grandscript RT Enzyme. Two no reverse transcriptase (NRT) control wells were used per gene. The program for reverse transcription is shown in Table B.1. Plate placed at -20°C after reaction.

The qPCR reaction mixture was prepared in new PCR plate, using 2 μ l cDNA to a 6 μ l reaction with 2x TATAA SybrGrand Master Mix. Primers used for the studied genes are presented in Table A.1. Three no template control (NTC) wells were used per gene. Eight reference genes were used: 18S, EIF1, RPS10, GAPDH, RPL7, EWSR1, YWHAZsh and RPS26. The program for qPCR reaction is shown in Table B.2.

3.4 Lentiviral transduction of K562 cells

Initially, the optimal blasticidin concentration for selection of untransduced cells was determined in two sets of experiments, clarified in Table 3.2. K562 and 721.221 cells were cultured in the presence of blasticidin (InVivoGen) at different concentrations and analyzed together with a negative control, cultured normally. The analysis was performed using a BD LSRFortessa and viability was based on cell morphology. The lowest concentration that killed all cells in the sample was regarded optimal.

Table 3.2: *Experiments for testing of optimal blasticidin concentration for selection.*

Experiment	Blasticidin concentrations ($\mu\text{g/ml}$)	Analysis after
1	1, 2.5, 5, 10	2 & 6 days
2	5, 10, 20, 30, 40, 50	6 days

Lentivirus was used to generate a cell line constitutively expressing *S. pyogenes* Cas9. Lentiviral prep particles (Addgene #52962-LV) produced from lentiCas9-Blast (Addgene plasmid #52962), deposited by Feng Zhang lab, were used for transduction of K562 cell line. An adapted spinoculation protocol was followed, given in Section B.2, and selection was performed using blasticidin. The untransduced control was analyzed using a BD LSRFortessa until all of the cells were dead. Blasticidin was then omitted from the medium and diluted in each cell split. Single cell sorting was performed on 1:5, 1:10 and 1:50 lentiviral dilutions in three 96-well plates, using a BD FACS ARIA. These were cultured with media changes based on colour change of medium. Polyclonal cells were cultured and frozen at several occasions. Around 30 wells had good growth after 10 days in monoclonal plates 1:5 and 1:10, but no cells in plate 1:50 did survive. After 18 days, the individual monoclonal cultures had reached around 1 million cells/ml in concentration. Out of these, 12 cultures from each plate were kept and cultured in 24-well plates. The remaining cells were frozen in the 96-well plates. Following this, 6 clones in total were kept in culture while the remaining were frozen.

3.5 Cas9 staining

To verify Cas9 expression, three separate stainings were performed using a Cas9 antibody. 100 000 cells were harvested, washed with buNaCl, permeabilized and fixed at room temperature for 30 min using Fixation & Permeabilization solution (Invitrogen) in 96-well plate. The cells were then stained at room temperature, in the dark for 30 min with Cas9 monoclonal antibody (10C11-A12, Invitrogen), diluted 1:100 in buNaCl in first two experiments and in Fixation & Permeabilization washing buffer in the last experiment. After washing with Fixation & Permeabilization washing buffer using centrifugation settings 500xg, 5 min, 20°C; fluorochrome-labelled secondary antibody (BV421 Rat anti-mouse IgG1, BD) was used to stain cells at room temperature for 30 min. The secondary antibody was diluted 1:160 in buNaCl in first two experiments and in Fixation & Permeabilization washing buffer in the last

experiment. Before analysis, the cells were washed with washing buffer and resuspended in elution buffer. Analysis was performed using a BD LSRFortessa. All six clones were analyzed in the first experiment, together with K562 wild-type, unstained control and secondary antibody control. In the second and third experiment, where different concentrations of the primary antibody were investigated, only the clone with highest expression in the first experiment was studied (10A11) together with controls.

3.6 Western Blot

Two different western blots were performed for further verification of Cas9 expression. The two western blots utilized either fluorochrome- or horseradish peroxidase (HRP)-coupled secondary antibodies for detection. Lysate was prepared of all six clones and the wild-type K562 cells (denoted negative control) by first washing 5 million harvested cells in buNaCl (centrifugation settings 350xg, 7 min, 4°C), followed by addition of 100 µl lysis buffer per sample, composed of 90 µl RIPA buffer (Sigma) and 10 µl protease inhibitor (Sigma-Aldrich). The suspension was mixed and incubated 5 min at 4°C. The samples were transferred to new tubes and centrifuged at 8000xg for 10 min at 4°C. The supernatants were collected and frozen at -80°C, except for 6 µl that was used to determine the protein concentrations. The western blots were prepared using NuPAGE Novex 4-12% Bis-Tris Protein Gel (Invitrogen). The frozen lysates were thawed on ice and diluted in dH₂O according to protein concentration measurements, based on the sample with lowest concentration. 13 µl lysate was mixed with 5 µl NuPAGE LDS Sample Buffer (Invitrogen) and 2 µl NuPAGE sample reducing agent (Invitrogen). The samples were heated to 70°C for 10 min, before loaded on the gel together with 5 µl Novex Sharp Pre-stained Protein Standard (Invitrogen). 800 ml NuPAGE MOPS SDS Running Buffer (Invitrogen) was used and 200 ml upper buffer, created from Running buffer with the addition of 500 µl NuPAGE antioxidant (Invitrogen). The gel was run for 50 min, 200 V and afterwards transferred to nitrocellulose membrane using iBlot (Invitrogen) which was blocked in different solutions for the two different western blots that were performed.

For the fluorochrome western, NaCl with 5% BSA was used for blocking 30 min and NaCl with 1% BSA was used for diluting the primary Cas9 antibody (10C11-A12, Invitrogen)(1:500) with two washing steps in dH₂O in between. The membrane was incubated with the primary antibody overnight at 4°C on a shaker. It was then washed twice with PBS/Tween followed by 1 h incubation with the secondary antibody (Donkey anti-mouse IRDye 800 CW), diluted 1:40 000 in Block Out solution (Rockland). The membrane was washed three times in PBD/Tween before being analyzed using Licor Odyssey Infrared Imager.

For the western using HRP-coupled secondary antibody, the membrane was first blocked for 30 min using WesternBreeze Blocker/Diluent (Part A and B) (Invitrogen) followed by incubation 1 h at room temperature with the primary antibody (10C11-A12, Invitrogen), diluted 1:500 in WesternBreeze Blocker/Diluent (Part A and B). The membrane was incubated at 4°C overnight. The membrane was washed

three times with PBS/Tween before being incubated with the secondary antibody (Polyclonal Rabbit anti mouse immunoglobulins/HRP), diluted 1:1000 in Western-Breeze Blocker/Diluent (Part A and B) for 1 h. It was washed in PBS/Tween twice and PBS once before being developed.

3.7 gRNA design

The designed gRNA insert contains: recognition site for restriction enzyme XhoI, stop codon for fluorescent protein, short spacer, poly A tail, spacer, U6 promoter, recognition sites for RE BbsI, gRNA scaffold and recognition site for restriction enzyme BamHI. The full gRNA insert sequence can be found in Section A.2. The sequence for the gRNA scaffold originates from the plasmid PX458 (pSpCas9(BB)-2A-GFP (PX458), Addgene, #48138). Recognition site for restriction enzyme (RE) BbsI was included upstream of the gRNA scaffold in the insert to enable ligation of a crRNA with compatible overhangs. Two crRNAs (20 bp) for NCR3LG1, PVR and NECTIN2, validated from Broad institute were chosen, given in Table 3.3. The 5'ends of the ordered oligomers were phosphorylated and a guanine (G) base was added in the overhang immediately upstream of the crRNA if not already present in the sequence, in order to increase ligation efficiency. Targeting of an early coding region, a common exon, high activity and minimal off-targets were considered the most important features in the choice of crRNA. The crRNAs were also confirmed using Synthego guide design verification tool (Web tool, Synthego). They are all located close to a 5' NGG 3' PAM sequence, needed for *S. pyogenes*. A more detailed description of the design procedure can be found in Section 4.5.

Table 3.3: *crRNA sequences for the genes NCR3LG1, PVR and NECTIN2.*

crRNA	Sequence (5'→3')
NCR3LG1_2	GTACCCATAGACGTGATGTTG
NCR3LG1_3	CACCAAGAGGCATTCCGACC
PVR_2	CGCAGGGGACGTCGTCGTGC
PVR_3	CCTGTTTCGTCACGTTCCCGC
NECTIN2_1	GGTCCGTCCGAGGGATGACC
NECTIN2_2	GCGAGTTCAAGTGCTACCCG

3.8 Plasmid construction

Plasmids were used for delivery of the gRNAs and are presented in Table 3.4. They were all obtained from Addgene, deposited by Michael Davidsons lab. The plasmids were chosen based on their fluorescent proteins (FPs) and what could be detected using the flow cytometers available in the lab.

3. Methods

Table 3.4: *Plasmids used in the current project. All were obtained from Addgene, deposited by Michael Davidsons lab.*

Plasmid	Fluorescent protein	Addgene cat. number
mEGFP-C1	EGFP; Excitation: 488, Emission: 507	#54759
EBFP2-C1	EBFP; Excitation: 383, Emission: 448	#54665
mPapaya1-C1	Papaya; Excitation: 530, Emission: 541	#54722
mCherry2-C1	Cherry; Excitation: 587, Emission: 610	#54563

The insert was ordered as a gblock from IDT. The crRNA oligomers, Table A.3, were received both in dried form and in lab ready TE buffer from IDT and oligomers NCR3LG1_2 and NCR3LG1_3 were resuspended in dH₂O to obtain concentration 100 μ M. Protocol for annealing of the oligomers can be found in Section B.3. The ordered plasmids were delivered as bacterial stabs that initially were used to create overnight cultures. Overnight cultures were generally created using 5 ml LB medium with 100 μ g/ml kanamycin and incubated overnight in shaker at 37°C. For midiprep kits, the volume LB medium was increased to 100 ml. Glycerol stocks were prepared using 500 μ l 50% glycerol and 500 μ l overnight culture. The glycerol stocks were frozen at -80°C and to recover the bacteria, a pipette tip was used to scrape off the top layer to create overnight culture. Plasmids were generally extracted using QIAprep Spin Miniprep Kit (Qiagen) and Plasmid Midi kit (Qiagen) was used for plasmid extraction needed for K562 transfection, when more concentrated DNA was required. Transformation was performed using ElectroMAX DH5 α -E Competent Cells and Subcloning Efficiency DH5 α Competent Cells (both Thermo Fisher Scientific). Protocols for both transformation methods were followed with the exception for ElectroMAX DH5 α -E Competent Cells in that DNA precipitation was not performed and the electroporator used was BioRads MicroPulser with pre-programmed Ec1 program (0,1 cm cuvette; 1,8 V; 1 pulse). For both competent cells, pUC19 control DNA (included with ElectroMAX cells) and undigested original plasmid were used as positive controls separately. Incubation in shaker for 1 h at 37°C in SOC medium (Thermo Fisher Scientific) was performed after transformation for both methods, followed by spreading on pre-warmed 100 μ g/ml kanamycin selective plates and incubation overnight at 37°C. For pUC19 control DNA, cells were spread on LB plates with added 100 μ g/ml ampicillin.

Digestions of the original plasmids and insert were performed using FastDigest BamHI and XhoI (Thermo Fisher Scientific) using the recommended conditions or in certain cases with extended incubation time of 10 min. Ligations were performed using T4 DNA ligase (New England Biolabs (NEB)) at recommended conditions or with extended incubation time of 30 min. Combined digestion and ligation for the crRNA oligomers and the plasmid+insert was performed with BbsI (NEB) and T4 DNA ligase (NEB). Protocol can be found in Section B.4. The two crRNAs for the same gene were inserted in plasmids with the same FP.

Purification of digested plasmids and insert was performed on 1% agarose gel using Takara RECOCHIP as recommended in protocol.

Restriction analysis with BbsI (NEB) was performed on all visible colonies and positive samples were chosen and verified by sequencing (Eurofins Genomics).

3.9 gRNA transfection of K562 cell line

Transfection of K562 was performed using the constructed plasmids mEGFP-C1+NCR3LG1 gRNA3, EBFP2-C1+PVR gRNA3. Electroporation was performed both with the separate plasmids as well as a combined plasmid sample, using the Neon transfection system (Thermo Fisher Scientific). The enclosed protocol for the Neon transfection system and the cell line-specific protocol for K562 cells were followed. The plasmids were purified using Qiagen midiprep kit, which gave concentrations 3066.4 ng/ μ l for mEGFP-C1+NCR3LG1 gRNA3 plasmid and 4397.0 ng/ μ l for EBFP2-C1+PVR gRNA3 plasmid. 15 μ g and 22 μ g of plasmid DNA were used in the separate samples respectively and the same amount of each plasmid in the combined sample. K562 cells were harvested and washed with buNaCl before being resuspended in Resuspension buffer R at a concentration of 1×10^7 . DNA and 100 μ l cell suspension was mixed and inserted in Neon transfection system using a 100 μ l tip. The parameters that were used are presented in Table 3.5. After transfection, the cell suspension was added to 2 ml pre-heated complete IMDM without antibiotics in a 6-well plate and incubated at 37°C. Analysis of transfection efficiency and viability was performed 48 h post transfection and single cell sorting of clones was performed 72 h post transfection.

Table 3.5: *Parameters for Neon transfection system used for transfection of K562 cell line.*

Pulse voltage (V)	Pulse width (ms)	Pulse number	Tip type
1 450	10	3	100 μ l

3.9.1 Analysis of transfection efficiency and viability

48h post transfection, 50 μ l cell suspension from cells transfected with mEGFP-C1+NCR3LG1 gRNA3 and EBFP2-C1+PVR gRNA3 was transferred to a facs tube and analyzed in a BD FACS ARIA. It was performed to study transfection efficiency, using GFP and BFP and viability, based on morphology. Wild-type K562 cells were used as negative control.

3.9.2 T7 Endonuclease I assay

To verify that the Cas9 endonuclease had in fact cleaved the genes of NCR3LG1 and PVR after transfection of the gRNAs, a T7 Endonuclease I (T7EI) assay was performed. The GeneArt Genomic Cleavage Detection Kit (Thermo Fisher Scientific) was used and the included protocol was followed. 1% agarose gel was used with the GeneRuler 1kb DNA ladder (Thermo Fisher Scientific). The PCR primers were designed using benchling (Benchling, Inc.) and are presented in Table A.2. A test PCR was run to ensure correct melting temperature and elongation time for the reaction and the program used in the assay can be seen in Table B.3. The assay was performed at day 2 and 6 post transfection, after a high transfection efficiency had been confirmed to avoid sorting of GFP/BFP-positive cells. Vague results were sent for sequencing (Eurofins Genomics), using the PCR product.

3.9.3 B7-H6 and PVR staining

To verify a reduced expression of the protein encoded by NCR3LG1, B7-H6, and PVR in monoclonal cells, staining of the proteins was performed. Single cells were sorted 72 h post transfection, based on their expression of FP, using a BD FACS ARIA. Three 96-well plates were prepared with 200 μ l complete IMDM medium and incubated at 37°C before sorting. Single cells transfected with mEGFP-C1+NCR3LG1 gRNA3, EBFP2-C1+PVR gRNA3 and combined both plasmids were sorted in each well in one 96-well plate with the last well being used as a control with 100 cells. The plates were incubated at 37°C immediately after sorting. 18 days after sorting, the cells were analyzed for the expression of B7-H6 and PVR. 25 μ l (~17 000 cells) from each well in each row was pooled into one sample. The cells transfected with both plasmids were used to make two separate samples that were stained separately for both proteins. The cells were washed twice in cold staining buffer (PBS supplemented with 0.5% BSA and 2 mM EDTA) and stained with primary antibodies for B7-H6 (17B1.3) and PVR (from Moretta lab) respectively. B7-H6 antibody was diluted 1:142 and PVR antibody 1:10, both in staining buffer. The cells were resuspended in 100 μ l primary antibody dilution and incubated at 4°C for 30 min. The cells were twice washed in cold staining buffer and incubated in 50 μ l goat serum, diluted 1:5 in staining buffer, for 10 min at 4°C. 50 μ l Goat anti-mouse Alexa Fluor 488 secondary antibody (Invitrogen A11001), diluted 1:500 in staining buffer, was added to the cell suspension and incubated 30 min at 4°C. The cells were washed twice in staining buffer and resuspended in 200 μ l staining buffer. Analysis was performed using a BD LSRFortessa.

4

Results & Discussion

The results obtained are presented in the current section. This is combined with a discussion around the implication of the result and what it meant for the continuation of the project.

4.1 NK cell cytotoxicity

The results from the cytotoxicity experiments using primary NK cells on K562 cell line are presented in Figure 4.1, shown as specific lysis of K562 cells. NK cells were purified from buffy coats and cultured overnight in complete RPMI medium. NK cells and K562 cells were incubated at an E/T ratio of 1:1 together with blocking antibodies for NK cell receptors NKp46, NKp30, NKp44, DNAM-1, 2B4 and CD2 for 4 hours, followed by live-dead stain and analysis using flow cytometry. Although there is great variation within the samples due to the small sample size (n=3), all receptors display an involvement in NK cell cytotoxicity. NKp30 and DNAM-1 were shown to be of large importance since blocking them individually resulted in a large general decrease in lysed K562 cells. This indicates that the most important ligands to knock out further on in the project would be B7-H6 (NCR3LG1 gene), ligand to NKp30, and PVR together with NECTIN2, which are ligands to DNAM-1.

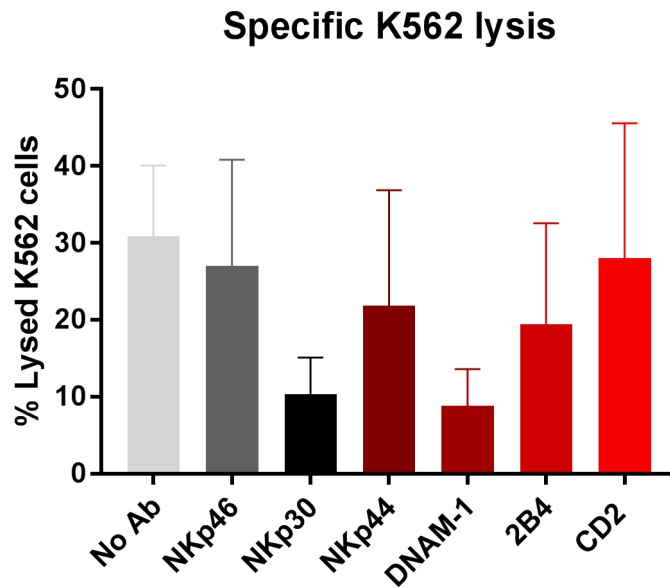


Figure 4.1: *Specific lysis of K562 cells with primary NK cells ($n=3$, error bars represent SEM). Blocking antibodies were used to block individual receptors on NK cells to study its effect on target cell lysis.*

4.2 Ligand expression using RT-qPCR

The result from the RT-qPCR showed that most analyzed ligands were expressed by both cell types. The amplification plots for the genes PVR, NECTIN2, MICA/MICB, ULBP1-3 are shown in Figure 4.2, in which expression for K562 cells are shown in dark green and 721.221 cells are shown in light green. All plots except for ULBP3 show that both cell types express that specific ligand. However, ULBP3 shows no expression which can be seen by the high cycle quantification (Cq) value. The amplification plots for the genes CD48, CD58, NCR3LG1, CLEC2B and BAG6 are displayed in Figure 4.3 and what can be seen is that CD58, NCR3LG1 and BAG6 are all expressed by both cell types. The gene for CLEC2B is, however, only expressed by K562 cells and CD48 is not expressed by any cells, again displayed by the high Cq value. A summary of the gene expression for both cell types is given in Table 4.1. The lack of ULBP3 expression in both cell lines is of valuable information for the future since it means that the knockout of that gene is not necessary if the goal is to reduce the effect of the NKG2D receptor in killing of these two cell lines. On the other hand, NKG2D has many other ligands that are expressed and that would be crucial to knockout in that event [38]. CLEC2B is only expressed by K562 and lacking in 721.221. It is the gene encoding the ligand for NKp80 and the lack of expression would therefore abolish the dependence on NKp80 for killing of 721.221 cells [39]. The lack of expression of CD48 in both cell types also reduce the dependence on the receptor 2B4 for activation and killing. The results from the cytotoxicity experiments showed a role for 2B4 in killing of K562 cells, which

is non-intuitive, based on the results presented here. This could however be due to undiscovered ligands for the receptor.

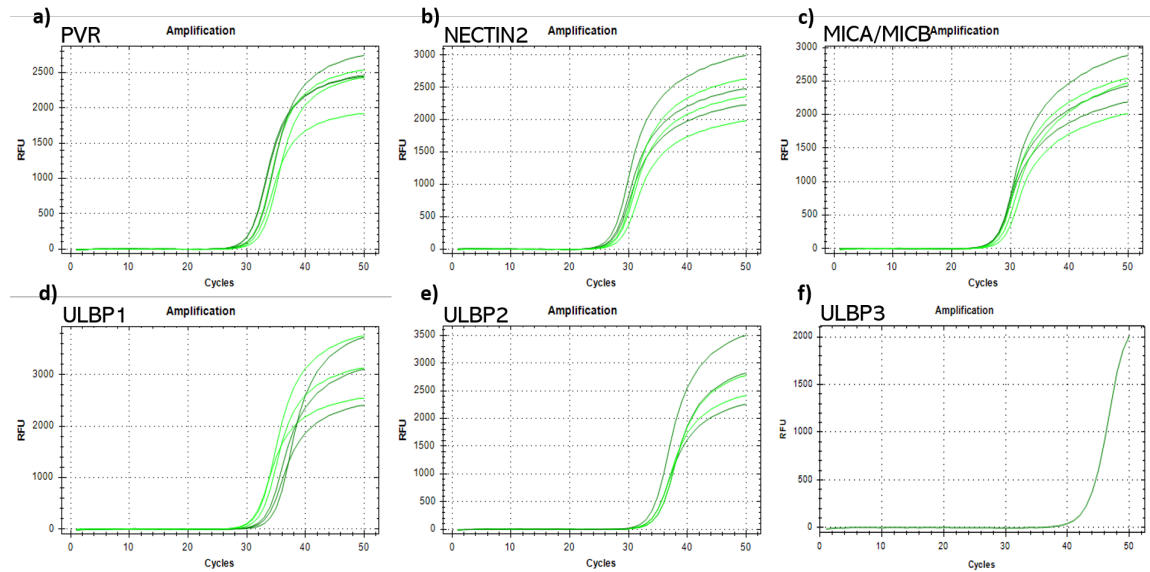


Figure 4.2: Amplification plots from RT-qPCR for genes a) PVR, b) NECTIN2, c) MICA/MICB, d) ULBP1, e) ULBP2 and f) ULBP3. K562 cells are shown in dark green and 721.221 cells are shown in light green.

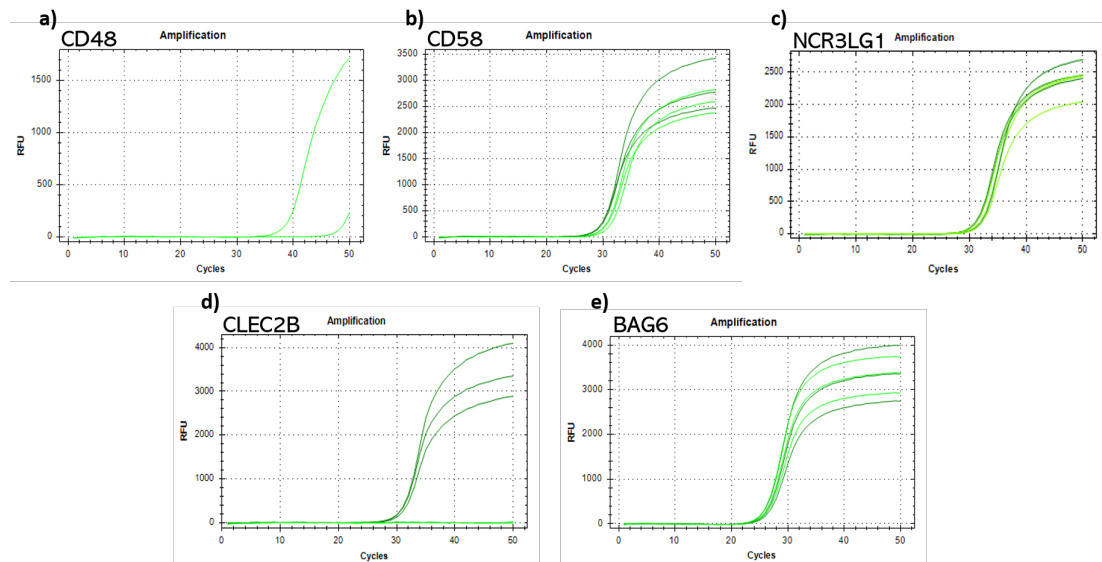


Figure 4.3: Amplification plots from RT-qPCR for genes a) CD48, b) CD58, c) NCR3LG1, d) CLEC2B and e) BAG6. K562 cells are shown in dark green and 721.221 cells are shown in light green.

The cytotoxicity experiments showed the importance of NKp30 and DNAM-1 in NK cell killing of K562 cells. Combined with the RT-qPCR result that verified expression of the ligand genes NCR3LG1 for NKp30 and PVR and NECTIN2 for

DNAM-1, it was confirmed that these would be the most important ligand genes to knock out, in order to obtain a higher dependency on NKp46 in killing of the cell line.

Table 4.1: Gene expression of ligands in K562 and 721.221 cells, studied by RT-qPCR. The symbol \checkmark indicates expression.

Ligands	K562	721.221
PVR	\checkmark	\checkmark
Nectin2	\checkmark	\checkmark
MICA/MICB	\checkmark	\checkmark
ULBP1	\checkmark	\checkmark
ULBP2	\checkmark	\checkmark
ULBP3		
CD48		
CD58	\checkmark	\checkmark
NCR3LG1	\checkmark	\checkmark
BAG6	\checkmark	\checkmark
CLEC2B	\checkmark	

4.3 Blasticidin experiments

To determine the optimal concentration of blasticidin to use for selection of transduced cells, two experiments were performed using different concentrations of blasticidin in culture with K562 cells. The results are presented in Figure 4.4 and show a high reduction in live cells when increasing the blasticidin concentration from 20 μ l/ml to 30 μ l/ml and not reduced markedly with higher concentrations, data not shown. Therefore, the concentration 30 μ l/ml was chosen to use for selection.

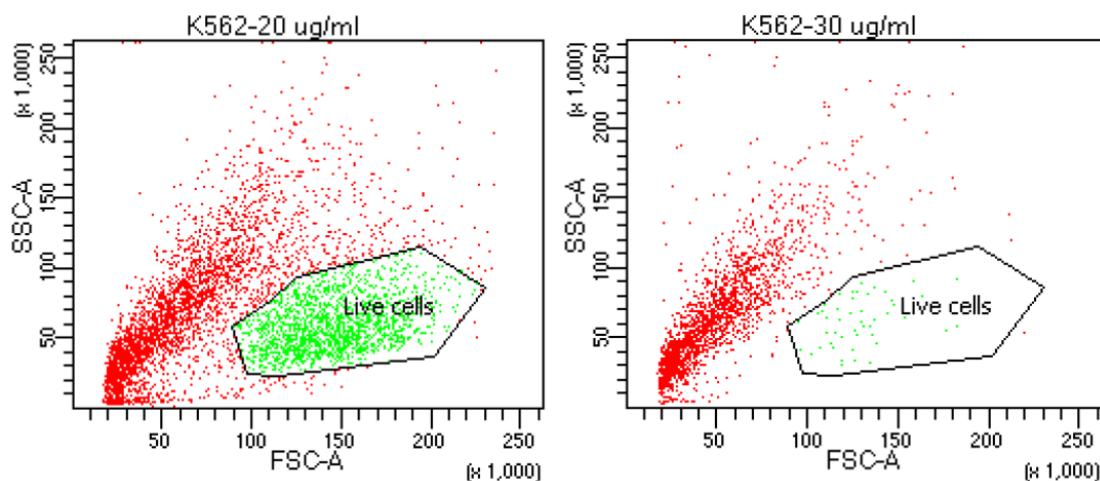


Figure 4.4: Experiment for determining the optimal blasticidin concentration for selection of transduced K562 cells. The images display the dot plots for cells cultured with 20 μ l/ml (left) and 30 μ l/ml (right) blasticidin respectively. The live cells are gated.

4.4 Verification of Cas9 expression

The K562 cell line was exposed to lentiviral prep particles containing Cas9 and single clones were established. The Cas9 expression in the six clones 5A2, 5A3, 5B10, 10A11, 10B7 and 10C8 was studied using two different methods.

4.4.1 Flow cytometry

The results from the flow cytometer analysis, presented in Table 4.2 show an increased expression in the 10A11 clone compared to the wild-type K562 cells. A too high concentration of the primary antibody was considered to be the reason for the high expression in the negative control. Therefore, the primary antibody was titrated using the clone with the highest expression, 10A11, and the K562 wild-type, with results presented in Table 4.3.

Table 4.2: *Median fluorescence intensity values of BV421 for Cas9 expression in six clones with unstained control, secondary antibody control and K562 wild-type control.*

Sample	Median fluorescence intensity
Unstained ctrl	834
Secondary Ab ctrl	1411
K562 wt ctrl	6318
5A2	7092
5A3	7835
5B10	7972
10A11	9020
10B7	7396
10C8	6963

Table 4.3: *Median fluorescence intensity values of BV421 in Cas9 primary antibody titration using clone 10A11 and K562 wild-type. Unstained control and secondary antibody control were included.*

Sample	K562 wt	10A11
Unstained ctrl	998	1041
Secondary Ab ctrl	1056	1115
1:100	4239	4668
1:200	2470	2978
1:400	1776	1883
1:800	1372	1518
1:1600	1145	1294

The results from the primary antibody titration showed a consistently higher expression of Cas9 in the 10A11 clone compared to the wild-type K562. The difference

between the wild-type and the clones was still considered too high to be fully convincing and therefore it was decided to confirm the results with western blot using the same primary antibody.

4.4.2 Western blot

The result from the western blot is presented in Figure 4.5. The band shown is at the correct size of the Cas9 protein - 160kDa. The result showed a high expression of the protein in clone 10A11 which confirms the previous results using flow cytometry. Clones 5A2, 5B10 and 10B7 were also shown to have lower expression of Cas9 and no expression was visible in the negative control.

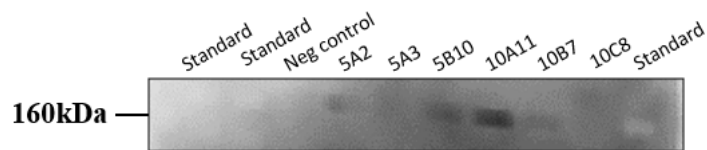


Figure 4.5: Results from Western blot for verification of Cas9 expression in six clones. As negative control, wild-type K562 was used.

The combined results from the flow cytometry experiments and the western blot confirms the positive result for the clone 10A11. Both methods show a high expression of the protein Cas9 which is a requirement for succeeding experiments. This clone was therefore chosen to use in the following experiments.

4.5 gRNA design

The first to consider regarding the gRNA design was what delivery system that would be appropriate. Since Cas9 was already expressed by the cell line, delivery of the gRNA alone was required. The two possibilities were to deliver it either simply as RNA or in a plasmid. The advantages of delivering it as RNA were the easier transfection step due to the smaller size and the less time consuming cloning steps required. However, the trouble with RNA not allowing selection of transfected cells which is required in order to co-transfect cells with several RNAs for several genes was a disadvantage. This possibility and the easier handling made a plasmid the preferred choice. A plasmid containing both a gRNA scaffold and *S. pyogenes* Cas9 that was already used in the lab was considered but would require removal of the Cas9 gene. The knockout experiments would also serve as a verification of the functionality of the Cas9 protein expressed by the cell line. The verification was required since the final genome-wide gRNA library does not contain the Cas9 protein.

As mentioned, transfection with several gRNAs would be preferred since it reduces the number of steps and therefore also the time consumption. The more gRNAs transfected simultaneously does however, reduce the likelihood of finding cells that

have been transfected with all gRNAs. A plasmid containing several gRNAs was regarded too large for transfection and using several selection markers was considered too tough on the cells. Instead, the use of several plasmids with different fluorescent markers that could enable detection of cells with all plasmids using flow cytometry was considered to be a better alternative. Plasmids with identical backbone allowed for incorporation of a designed insert containing the gRNA for each specific gene. In the design of the insert, the crRNA was coupled to a gRNA scaffold that contained the binding site for *S. pyogenes* Cas9. The promoter used in the first design was U6. Since the multiple cloning site (MCS) was located downstream of the FP, a polyA tail was added before the U6 promoter, separated by a spacer sequence. Later in the process it was discovered that the MCS was also in frame with the FP, as also a stop codon was incorporated into the insert upstream of the polyA tail, again separated by a short spacer sequence. The plan to order the insert as two oligomers required overhangs on the end, based on the choice of restriction enzymes (REs) to allow for plasmid ligation. Common REs were chosen with recognition sites present in MCS of the chosen plasmids but not present in the insert which could allow for simultaneous digestion and ligation.

Since the insert was far over 200 bp long which is the maximum limit for long oligomers provided by most companies, options for shortening of the construct was searched for. Kennedy et al. [40] showed the possibility to use a much shorter tRNA promoter (72 bp) instead of U6 (241 bp). This resulted in a significantly shorter fragment but still too long for an oligomer (237 bp).

The chosen strategy was instead to order the insert as a gblock, which is a dsDNA fragment that could be synthesized much longer. With no length restriction, the U6 promoter was chosen as it was more well-known and sites for REs were added to the ends of the gblock to create the correct overhangs. As it would be more economic to only exchange the specific crRNA for each gene instead of synthesizing a new insert, sites for RE were included upstream of the gRNA scaffold and the crRNAs were designed with compatible overhangs. The final designs are presented in Figures 4.6 and 4.7.

Insert U6 prom. (428 bp)

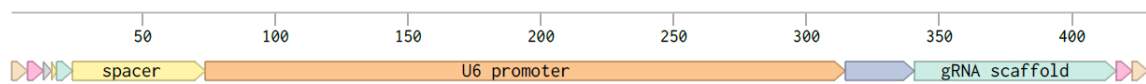


Figure 4.6: *Insert for gRNA in form of gblock. The design include from left to right: 6 bp from end for RE, recognition site for RE XhoI, stop codon for FP, short spacer, poly A tail, spacer, U6 promoter, recognition sites for RE BbsI, gRNA scaffold, recognition site for RE BamHI and 6 bp from end for RE.*

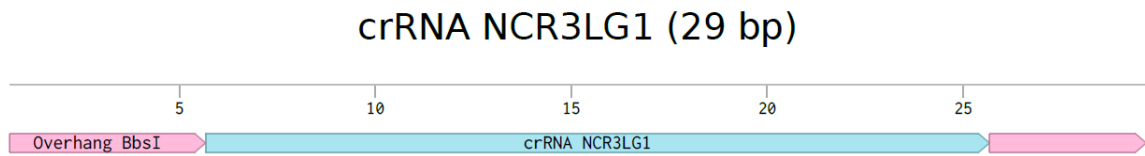


Figure 4.7: *crRNA for the gene NCR3LG1 with overhangs for RE BbsI digestion.*

4.6 Verification of gRNA transfection

Cell viability and transfection efficiency was studied 48 h and 72 h post transfection using flow cytometry. The results from studies of transfection with mEGFP-C1+NCR3LG1 gRNA3, EBFP2-C1+PVR gRNA3 and double transfection with both plasmids are shown in Figures 4.8, 4.9 and 4.10 respectively. The first dot plots display the gating of the live and the dead cells. The live cells are then studied in the histogram to the right where the GFP/BFP-positive cells have been gated. The histograms have an overlay of the control cells, shown in grey. Table 4.4 summarizes the results. A high transfection efficiency as well as viability was shown. Since the efficiency was high, it was decided to proceed with the T7EI assay with the polyclonal cells without sorting them first. Too low transfection efficiency would mean too few cells with potential mismatched DNA for detection to be possible with the T7EI assay.

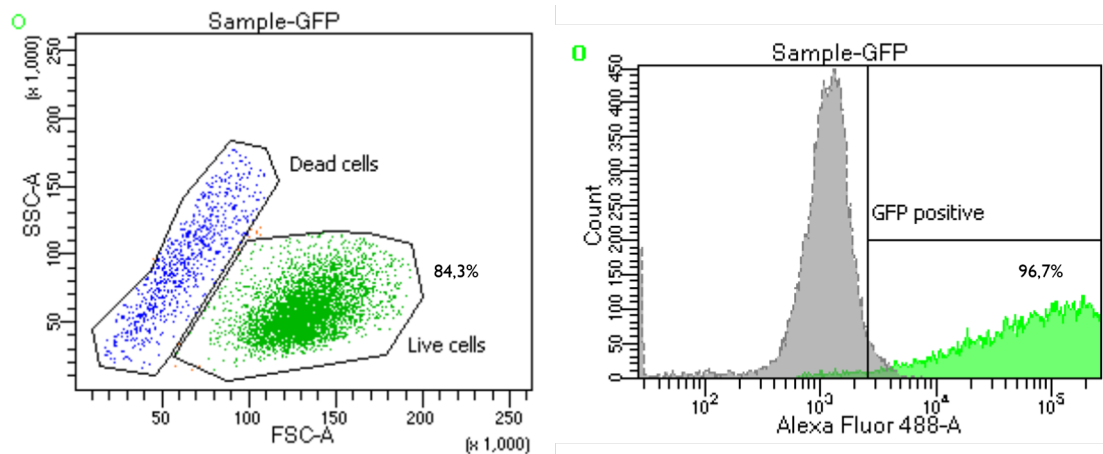


Figure 4.8: *Cell viability and transfection efficiency results from K562 transfection with mEGFP-C1+NCR3LG1 gRNA3 plasmid 48h post transfection.*

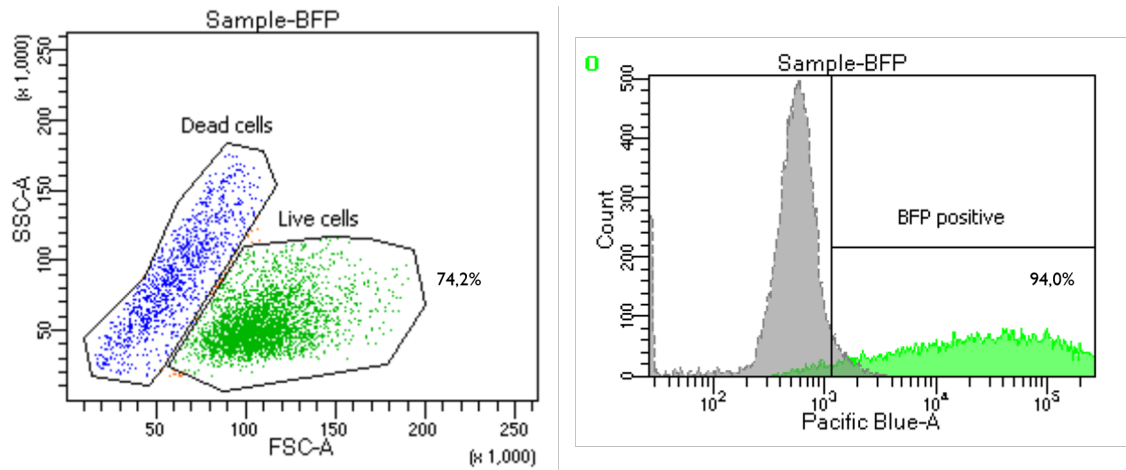


Figure 4.9: Cell viability and transfection efficiency results from K562 transfection with EBFP2-C1+PVR gRNA3 plasmid 48 h post transfection.

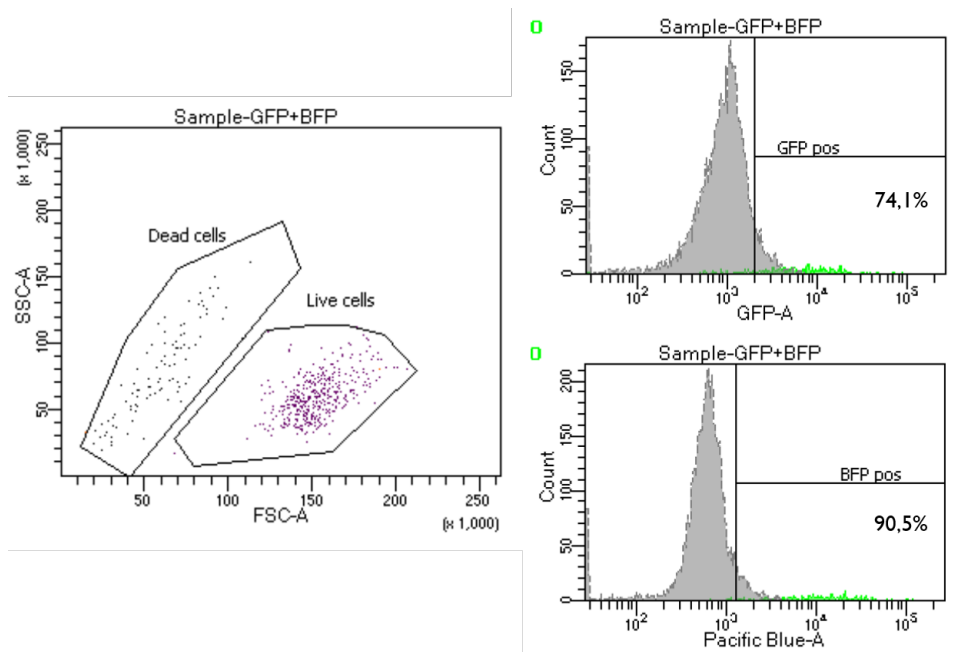


Figure 4.10: Cell viability and transfection efficiency results from K562 transfection with mEGFP-C1+NCR3LG1 gRNA3 and EBFP2-C1+PVR gRNA3 plasmids 72 h post transfection.

Table 4.4: Result from transfection of K562, obtained using flow cytometry 48 h and 72 h post transfection.

Sample	Cell viability	Transfection efficiency
mEGFP-C1 + NCR3LG1 gRNA3	84,3%	96,7%
EBFP2-C1 + PVR gRNA3	74,2%	94,0%
Double transfection	79,8%	74,1% (GFP), 90,5% (BFP)

4.7 Verification of functional Cas9 and cleavage of genes

Cas9 was shown to be functional using the T7EI endonuclease assay at day 6 post transfection. The resulting gel image is displayed in Figure 4.11 and it shows the well for NCR3LG1 gRNA3 to the left with the negative control to the right. The well with NCR3LG1 gRNA clearly show two bands below the parent band which confirms the cleavage of the gene as a result of mismatched DNA. This does in turn confirm the functionality of the Cas9 expressed by the cell line.

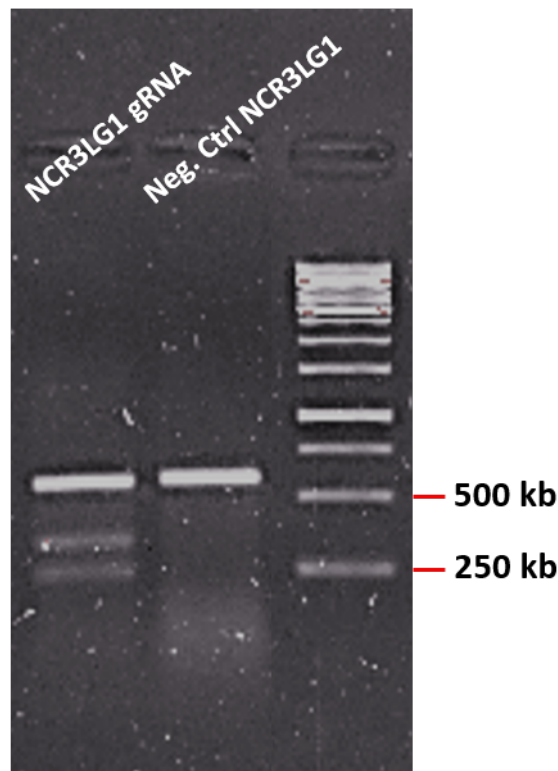


Figure 4.11: Result from T7EI assay, performed 6 days post transfection with gRNAs for NCR3LG1 and PVR genes. The visible fragments verifies Cas9 functionality.

The T7EI result from day 6 is shown in Figure 4.12 and the ladder used is GeneRuler 1kb. The result for plasmid mEGFP-C1 + NCR3LG1 gRNA3 is shown in the well furthest to the left and the two bands below the parent band confirm the correct cleavage of the gene. The parent band should be 573 bp long and the cleaved fragments should be of the lengths 335 bp and 238 bp.

The result for the PVR gRNA3 is not as clear. The parent band should be 855 bp long and the cleaved bands should be 597 bp and 258 bp. The bands visible for PVR sample and control at around 300-400 bp, both for samples with enzyme and negative enzyme control are believed to be due to unspecific primer binding in PCR reaction and annealing temperature could potentially be elevated. The fact that there is a band visible at around 700 bp for both the PVR sample and the negative

PVR control with added enzyme which is not present for the negative enzyme-control could be due to differences in the sequence between the two PVR genes in the cells. This would also be recognized as a mismatch by the T7 endonuclease. The parent band is considerably weaker than for NCR3LG1 gRNA3 which might result in too weak cleaved bands to distinguish. The positive control also have substantially weaker bands, which might imply generally too low amounts of DNA to be able to distinguish the bands. Therefore it is difficult to confirm that no cleavage in the PVR gene has occurred in any cells. The amount of cells with cleaved genes might be too low to distinguish in this assay but it could be possible to recognize in the individual clones.

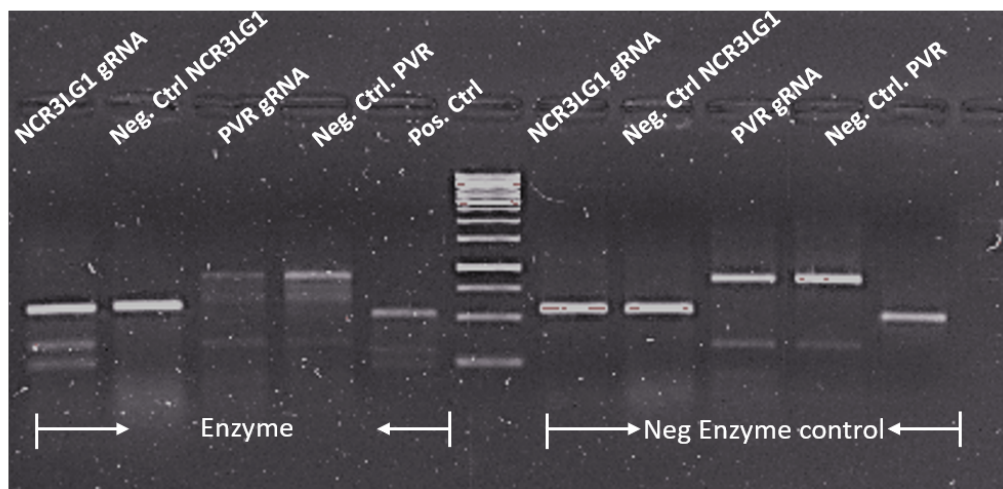


Figure 4.12: Gel electrophoresis result from T7EI assay, performed 6 days after transfection with gRNAs for NCR3LG1 and PVR genes.

4.8 Verification of reduced expression of B7-H6 and PVR

Flow cytometry was used to verify a reduced expression of B7-H6 and PVR in the monoclonal cells, created by single-cell sorting in three 96-well plates. Each row in the plates was pooled in the first experiment and from the result, one row from each plate with four extra wells for B7-H6 and PVR were chosen based on a low general expression. In the new experiment, each clone in the chosen rows was stained. Seven clones that had a lower expression than the positive control were chosen from each plate to be expanded for further verification in the future. The results for all B7-H6 stainings are shown in Figure 4.13.

The results for the pooled experiment, left in Figure 4.13, showed a low expression in all pooled samples which was surprising since it was not expected to be that many clones with a reduced expression. The sample with the broadest peak, sample B, was therefore chosen for study of individual clones. It was considered more reasonable that there was a broader distribution within the sample. For assurance, four wells from the sample with clearly the lowest expression, sample H, were also included in the following experiment. The results from the individual stainings, both to the right in Figure 4.13, displayed varied protein expression where all types of expression can be seen. B1 display expression similar to the positive control which show a unsuccessful knockout of the gene of interest. B10 instead, display an intermediate expression which could indicate a knockout of one of the alleles and B5 display an expression comparable with the negative control and therefore it indicates a knockout of both alleles. The lowest protein expression is displayed by the seven clones B5, B6, B7, B9, B10, H9. The clones B3, B4, B8 and B12 are not displayed due to too low amounts of cells.

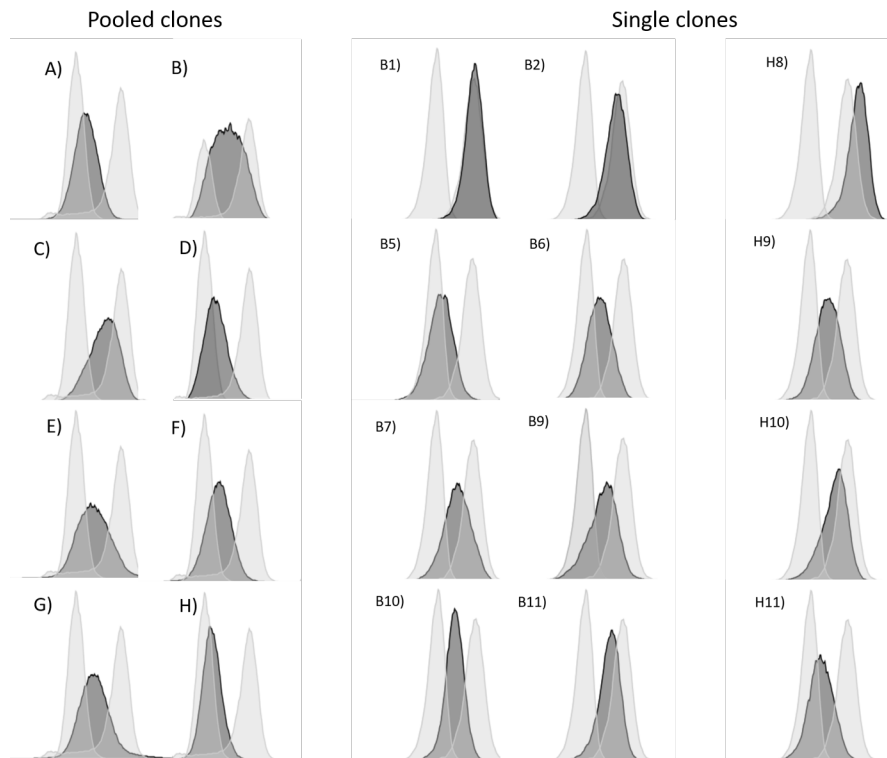


Figure 4.13: Histograms showing Alexa Fluor 488 intensity from staining of B7-H6 in gRNA-transfected K562 cells. Left histograms (A-H) show the pooled clones from all rows. Middle histograms show the single clones from row B and the right histograms show four clones from row H. The negative and the positive controls are displayed as grey peaks in all histograms and the samples are displayed as a black peak.

The result from all PVR stainings for the single transfected cells are displayed in Figure 4.14. The result from the pooled experiment, left in Figure 4.14, showed a generally low expression in most pooled samples. Based on a first analysis, row A was chosen for study of individual clones, together with four wells from row D. Sample A was chosen due to the broad peak and sample D due to the lowest expression. With further analysis with the overlay plots displayed here, another row than A might have been chosen since rows like B and E also had a broad curve but with a lower expression. The results from the individual stainings, both to the right in Figure 4.14, also showed a varied expression, with the lowest expression was found in clones A5, A10, A11, A12, D1, D2 and D3. Clones A6 and A9 are not shown here due to too low amount of cells.

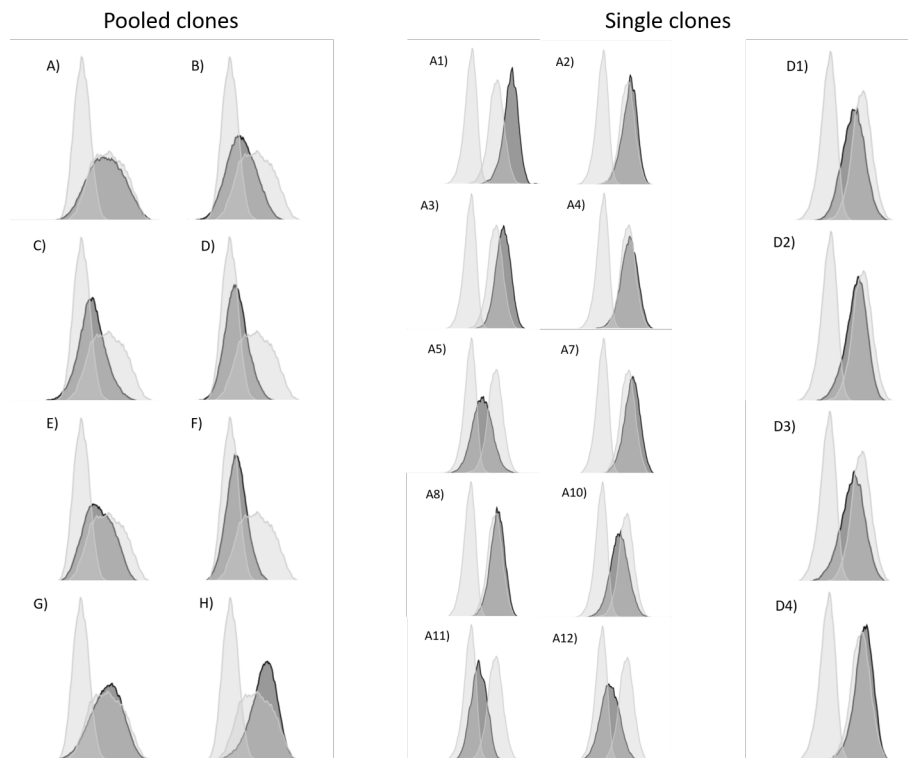


Figure 4.14: Histograms showing Alexa Fluor 488 intensity from staining of PVR in gRNA-transfected K562 cells. Left histograms (A-H) show the pooled clones from all rows. Middle histograms show the single clones from row A and right histograms show four clones from row D. The negative and the positive controls are displayed as grey peaks in all histograms and the samples are displayed as a black peak.

The results from the pooled samples for the doubly transfected cells, stained for B7-H6 and PVR, are shown in Figure 4.15. The same clones were used in two separate stainings for B7-H6 and PVR separately. The positive control for the PVR staining is very broad which makes analysis more difficult. Row C was chosen for individual staining since it visually has the lowest expression for both stainings. The results from the individual stainings for both B7-H6 and PVR are displayed in Figure 4.16. The clones C3, C4, C6, C7, C10 and C12 all have somewhat lower expression than the positive control but clone C5 show an almost complete absence of both proteins.

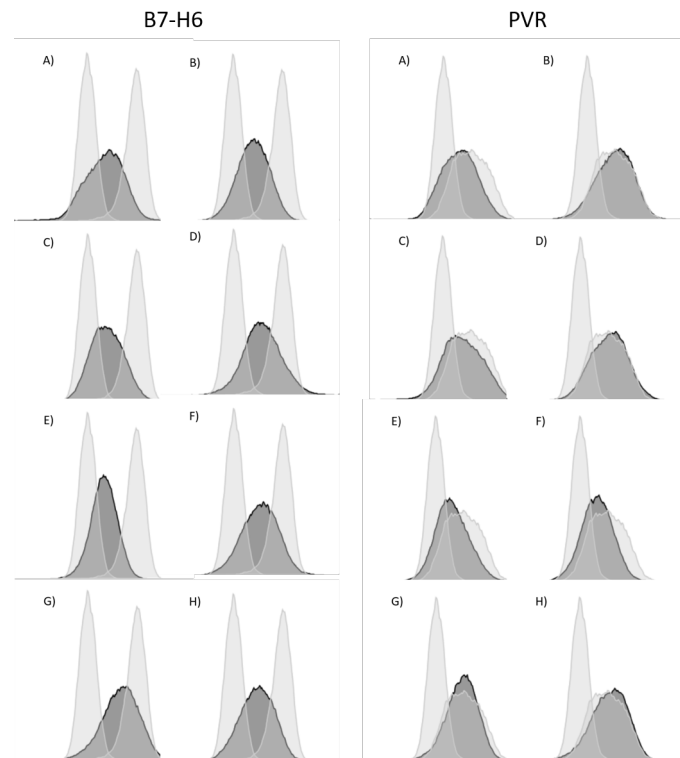


Figure 4.15: Histograms showing Alexa Fluor 488 intensity from staining of B7-H6 and PVR in doubly gRNA-transfected K562 cells. Histograms (A-H) show the pooled clones from all rows. The left histograms show the B7-H6 stained pooled clones and the right histograms show the same clones, stained for PVR. The negative and the positive controls are displayed as grey peaks in all histograms and the samples are displayed as a black peak.

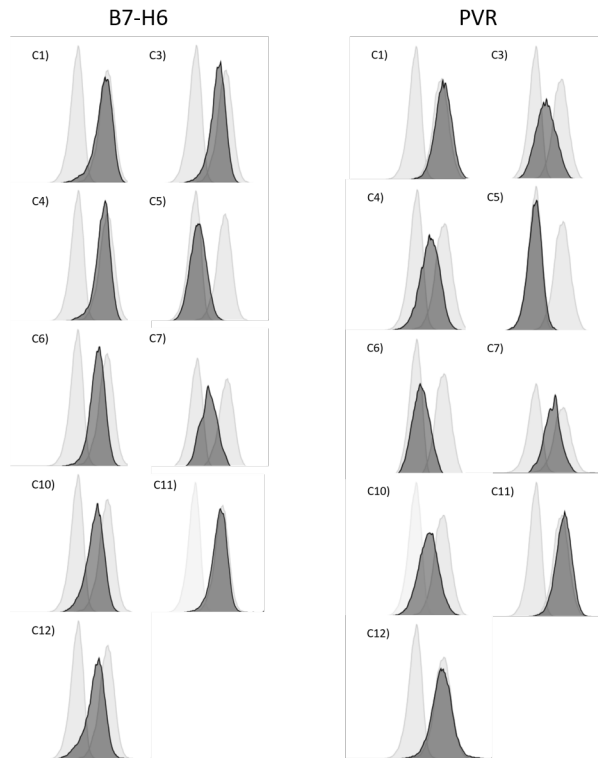


Figure 4.16: Histograms showing Alexa Fluor 488 intensity from staining of B7-H6 and PVR in doubly gRNA-transfected K562 cells. Histograms (A-H) show the single clones from row C. The left histograms show the B7-H6 stained clones and the right histograms show the same clones, stained for PVR. The negative and the positive controls are displayed as grey peaks in all histograms and the samples are displayed as a black peak.

The clones with the lowest expression were expanded and frozen to enable analysis for further verification by sequencing at a later stage. These clones will later be the ones that will be used for the following stages in the project.

5

Conclusion

To conclude, it has been proven successful to use a CRISPR approach to manipulate the NK cell receptor ligand expression in the K562 cell line.

This was achieved by completing the needed intermediate aims. The first aim was to define receptors involved in NK cell cytotoxicity of K562 cell line. The results have shown the importance of the activating receptors NKp30 and DNAM-1 in elimination of the K562 cell line and their ligands B7-H6, PVR and NECTIN2 were shown to be expressed by the cells.

The second intermediate aim included the generation of a Cas9-expressing K562 cell line and the results have shown the successful incorporation of Cas9 in the K562 cell line using a lentiviral vector and the verification of the protein expression using flow cytometry and western blots.

The third and fourth aim involved designing and generating gRNAs for knockout of ligands involved in NK cell cytotoxicity of the K562 cell line and creating a K562 cell line with selected ligand genes knocked out. The designed NCR3LG1 gRNA3 was generated and shown to function together with the Cas9, expressed by the engineered K562 cell line, and successfully cleave and mutate the NCR3LG1 gene. The resulting B7-H6 expression was shown to be reduced compared to untransduced control cells. Results for PVR show promise but must be verified further.

Bibliography

- [1] Torre LA, Bray F, Siegel RL, Ferlay J, Lortet-Tieulent J, Jemal A. Global cancer statistics, 2012. *CA: a cancer journal for clinicians*. 2015;65(2):87–108.
- [2] World Health Organization (WHO). *Cancer Fact Sheet*; 2018.
- [3] Blattman JN, Greenberg PD. Cancer immunotherapy: a treatment for the masses. *Science*. 2004;305(5681):200–205.
- [4] Cheng M, Chen Y, Xiao W, Sun R, Tian Z. NK cell-based immunotherapy for malignant diseases. *Cellular & molecular immunology*. 2013;10(3):230.
- [5] Caligiuri MA. Human natural killer cells. *Blood*. 2008;112(3):461–469.
- [6] Moretta A, Bottino C, Vitale M, Pende D, Cantoni C, Mingari MC, et al. Activating receptors and coreceptors involved in human natural killer cell-mediated cytotoxicity. *Annual review of immunology*. 2001;19(1):197–223.
- [7] Alberts B, Johnson A, Lewis J, Raff M, Roberts K, Walter P. *Molecular biology of the cell*. new york: Garland science; 2002. Classic textbook now in its 5th Edition. 2002;.
- [8] Vivier E, Raulet DH, Moretta A, Caligiuri MA, Zitvogel L, Lanier LL, et al. Innate or adaptive immunity? The example of natural killer cells. *Science*. 2011;331(6013):44–49.
- [9] Brauner A. *Medicinsk mikrobiologi & immunologi*. Studentlitteratur; 2015.
- [10] Murphy K, Weaver C. *Janeway’s immunobiology*. Garland Science; 2017.
- [11] Abbas AK, Lichtman AH, Pillai S. *Cellular and Molecular Immunology E-Book*. Elsevier Health Sciences; 2014.
- [12] Coico R, Sunshine G. *Immunology: a short course*. John Wiley & Sons; 2015.
- [13] Paul WE. *Fundamental Immunology*. Wolters Kluwer; 2012.
- [14] Yokoyama WM, Kim S, French AR. The dynamic life of natural killer cells. *Annu Rev Immunol*. 2004;22:405–429.
- [15] Martner A, Rydström A, Riise RE, Aurelius J, Anderson H, Brune M, et al. Role of natural killer cell subsets and natural cytotoxicity receptors for the outcome of immunotherapy in acute myeloid leukemia. *Oncoimmunology*. 2016;5(1):e1041701.
- [16] Janeway Jr CA, Travers P, Walport M, Shlomchik MJ. *The complement system and innate immunity*. 2001;.
- [17] *On the immunobiology of the natural killer cells*. 1981;.
- [18] Vilches C, Parham P. KIR: diverse, rapidly evolving receptors of innate and adaptive immunity. *Annual review of immunology*. 2002;20(1):217–251.
- [19] Yokoyama WM, Kim S. Licensing of natural killer cells by self-major histocompatibility complex class I. *Immunological reviews*. 2006;214(1):143–154.

- [20] Kim S, Poursine-Laurent J, Truscott SM, Lybarger L, Song YJ, Yang L, et al. Licensing of natural killer cells by host major histocompatibility complex class I molecules. *Nature*. 2005;436(7051):709.
- [21] Brandt CS, Baratin M, Eugene CY, Kennedy J, Gao Z, Fox B, et al. The B7 family member B7-H6 is a tumor cell ligand for the activating natural killer cell receptor NKp30 in humans. *Journal of Experimental Medicine*. 2009;206(7):1495–1503.
- [22] Nakajima H, Cella M, Langen H, Friedlein A, Colonna M. Activating interactions in human NK cell recognition: the role of 2B4-CD48. *European journal of immunology*. 1999;29(5):1676–1683.
- [23] Friberg DD, Bryant JL, Whiteside TL. Measurements of natural killer (NK) activity and NK-cell quantification. *Methods*. 1996;9(2):316–326.
- [24] Andersson LC, Nilsson K, Gahnberg CG. K562—a human erythroleukemic cell line. *International journal of cancer*. 1979;23(2):143–147.
- [25] Shimizu Y, DeMars R. Production of human cells expressing individual transferred HLA-A,-B,-C genes using an HLA-A,-B,-C null human cell line. *The Journal of Immunology*. 1989;142(9):3320–3328.
- [26] Rieseberg M, Kasper C, Reardon KF, Scheper T. Flow cytometry in biotechnology. *Applied microbiology and biotechnology*. 2001;56(3-4):350–360.
- [27] Jahan-Tigh RR, Ryan C, Obermoser G, Schwarzenberger K. Flow cytometry. *The Journal of investigative dermatology*. 2012;132(10):e1.
- [28] Albani JR. Structure and dynamics of macromolecules: absorption and fluorescence studies. Elsevier; 2004.
- [29] G MM. Flow Cytometry: Principles and Applications. Humana Press; 2007.
- [30] Naeem A, James N, Tanvir M, Marriam M, Nathaniel S. Fluorescence Activated Cell Sorting (FACS): An Advanced Cell Sorting Technique. *PSM Biological Research*. 2017;2(2):83–88.
- [31] Marcusson-Ståhl M, Cederbrant K. A flow-cytometric NK-cytotoxicity assay adapted for use in rat repeated dose toxicity studies. *Toxicology*. 2003;193(3):269–279.
- [32] Alter G, Malenfant JM, Altfeld M. CD107a as a functional marker for the identification of natural killer cell activity. *Journal of immunological methods*. 2004;294(1-2):15–22.
- [33] Carson M Sue, Witherow. Molecular biology techniques: A classroom laboratory manual. Academic Press; 2012.
- [34] Starkey M, Elaswarapu R. Genomics: essential methods. John Wiley & Sons; 2011.
- [35] Zhang F, Wen Y, Guo X. CRISPR/Cas9 for genome editing: progress, implications and challenges. *Human molecular genetics*. 2014;23(R1):R40–R46.
- [36] Vouillot L, Thélie A, Pollet N. Comparison of T7E1 and surveyor mismatch cleavage assays to detect mutations triggered by engineered nucleases. *G3: Genes, Genomes, Genetics*. 2015;5(3):407–415.
- [37] Zischewski J, Fischer R, Bortesi L. Detection of on-target and off-target mutations generated by CRISPR/Cas9 and other sequence-specific nucleases. *Biotechnology advances*. 2017;35(1):95–104.

- [38] Nausch N, Cerwenka A. NKG2D ligands in tumor immunity. *Oncogene*. 2008;27(45):5944.
- [39] Kuttruff S, Koch S, Kelp A, Pawelec G, Rammensee HG, Steinle A. NKp80 defines and stimulates a reactive subset of CD8 T cells. *Blood*. 2009;113(2):358–369.
- [40] Kennedy EM, Kornepati AV, Mefferd AL, Marshall JB, Tsai K, Bogerd HP, et al. Optimization of a multiplex CRISPR/Cas system for use as an antiviral therapeutic. *Methods*. 2015;91:82–86.

A

Appendix 1

A.1 Primers

Table A.1: *Primers used for RT-qPCR.*

Primer	Sequence (5'→3')
PVRv3_F	GTGGACGGCAAGAATGTGAC
PVRv3_R	ATCATAGCCAGAGATGGATACCT
NECTIN2_F	GAGGACGAGGGCAACTACAC
NECTIN2_R	TGGTTCTTGGGCTTGGCTAT
MICA/MICB_F	AAGGACCAGAAAGGAGGCTT
MICA/MICB_R	TCCCCATCGTAGTAGAAATGC
ULBP1v2_F	GGCAGATGAGGAGAGTTGTTT
ULBP1v2_R	AGGACCCAGACCAGGCTAAC
ULBP2_F	CGCTACCAAGATCCTTCTGTG
ULBP2_R	AAGAGAGTGAGGGTCCGGC
ULBP3_F	CGCTCCTGGTCTACAATGGC
ULBP3_R	TCTGGGCAAATGAATGATGGTG
CD48v3_F	GAGCAGCAAGAATGGCACG
CD48v3_R	TCATCTCAGGTAAGTAACAGGC
CD58v1_F	GTTCTTTCTTTATGTGCTTGAGTCT
CD58v1_R	TGGCTGTTGTAATGCTCTGGT
NCR3LG1v1_F	GCTGACGACCGAAGGTGAT
NCR3LG1v1_R	GTGATGTTGAGGGGTTGGGA
CLEC2Bv5_F	CCACTCAACATGCCGACCTA
CLEC2Bv5_R	TGCCATCTTCAGTCCAATCCA
BAG6_F	CACCCAACCATCCTTCCCCT
BAG6_R	CACCCAGAACCTCGTAGTAGC

Table A.2: *PCR primers used for T7 Endonuclease I assay.*

Primer	Sequence (5'→3')
NCR3LG1_F	CCTCCAGATACCATCACACT
NCR3LG1_R	AAGTGGAGCTCAAAGAGGTG
PVR_F	AGTGATGTTGAGATTCAGGG
PVR_R	AGATCTCTGCTTTCTTCCTG

A.2 Designed gRNA insert sequence

1 tgctgtctcg agtaagtaat aaacgttgct taactctat cggccgatt cgtattagct cggcgatec gtcgaggcc
 81 tatttccat gattcctca tatttcata tacgatacaa ggctgtaga gagataattg gaattaattt gactgtaaac
 161 acaaagatat tagtacaanaa tacgtgacgt agaaagtaat aatttcttg gtagttgca gttttaaata tatgtttta
 241 aatggactat catatgctta ccgtaacttg aaagtattc gatttcttg cttatataat cttgtggaaa ggacgaaaca
 321 ccgggtcttc gagaagacct gtttagagc tagaaatagc aagttaaaat aaggctagtc cgttatcaac ttgaaaaagt
 401 ggcaccgagt cggtcggat ccgtcgta

A.3 crRNA oligomers

Table A.3: *crRNA oligomers. The underlining show the complementary part.*

crRNA	Sequence (5'→3')
NCR3LG1_2	<u>CACCGTACCCATAGACGTGATGTTG</u>
NCR3LG1_2 rev. comp.	AAACCAACATCACGTCTATGGGTAC
NCR3LG1_3	<u>CACCGCACCAAGAGGCATTCCGACC</u>
NCR3LG1_3 rev. comp.	AAACGGTCGGAATGCCTCTTGGTGC
PVR_2	<u>CACCGCGCAGGGGACGTCGTCGTGC</u>
PVR_2 rev. comp.	AAACGCACGACGACGTCCCCTGCGC
PVR_3	<u>CACCGCCTGTTTCGTCACGTTCCCGC</u>
PVR_3 rev. comp.	AAACGCGGGAACGTGACGAACAGG
NECTIN2_1	<u>CACCGGTCCGTCCGAGGGATGACC</u>
NECTIN2_1 rev. comp.	AAACGGTCATCCCTCGGACGGACC
NECTIN2_2	<u>CACCGCGAGTTCAAGTGCTACCCG</u>
NECTIN2_2 rev. comp.	AAACCGGGTAGCACTTGAACTCGC

B

Appendix 2

B.1 RT-qPCR programs

Table B.1: *Program for reverse transcription.*

Temperature	Time
22°C	5 min
42°C	30 min
85°C	5 min
4°C	Forever

Table B.2: *Program for qPCR.*

Temperature	Time	Cycles
95°C	2 min	1 X
95°C	5 sec	
60°C	20 sec	49 X
70°C	20 sec	

B.2 Spinoculation protocol

1. Prepare DMEM Complete: 10% FBS and 4mM L-alanyl-L-glutamine.
2. Prepare a batch of DMEM complete + 5µg/ml polybrene.
3. Prepare a batch of cells as follows: Dilute 350,000 cells into a total volume of 7 ml of DMEM complete + 5µg/mL polybrene: Count cells, take 350 000 cells, add buNaCl, spin down and resuspend in new polybrene media. Mix well by pipetting or inverting the tube.
4. Rapidly thaw the lentiviral aliquot at room temperature.
5. Prepare dilutions 0, 1:5, 1:10, 1:50, 1:100 and 1:500 of the lentivirus in 37°C in DMEM complete + 5µg/ml polybrene with total volume of 0,5ml in 10ml tubes.
6. Aliquot 0,5 ml of cell suspension (i.e., 25,000 cells) into each tube. Mix by pipetting carefully.
7. Spin tubes 30min, 800g, 32°C in centrifuge.
8. Following centrifugation, remove tubes from centrifuge and transfer cells to a 24-well plate. Incubate at 37°C for 3h.

9. After 3h, “feed” cells with 0,5ml/well additional complete DMEM medium without polybrene. Incubate 24h.
10. After 24h, centrifuge cells in tubes and resuspend cells in 1,5 ml DMEM medium without polybrene. Transfer back to new wells on 24-well plate.
11. Incubate plate 2 days at 37°C.
12. Prepare DMEM complete + blasticidin with concentration 30µl/ml.
13. After 2 days, move the cells to 10ml tubes, centrifuge (200g, 5min), remove supernatant and dispose of appropriately (can contain virus) and resuspend pellet in 1,5ml DMEM complete + 30µl/ml blasticidin. Transfer cells back to 24-well plate.
14. Observe the dish every day to ensure that the cells in the untransduced well (0µl lentivirus, above) are dying. Perform regular fluid changes and monitor the growth of the cells.

B.3 Annealing of oligomers

1. Mix
 - 1µl of each oligomer
 - 1µl T4 DNA ligation buffer (NEB)
 - 7µl dH₂O
2. Incubate in thermocycler with program ranging from 95°C to 25°C with 10°C decrease each 10 min.

B.4 Combined digestion and ligation

1. Mix
 - 100ng plasmid DNA
 - 1µl annealed crRNA
 - 1µl 10X T4 ligation buffer (NEB)
 - 1µl 10X FastDigest buffer (NEB)
 - 1µl T4 DNA ligase (NEB)
 - 0,5µl BbsI (NEB)
 - dH₂O to total volume 10µl
2. Incubate at 37°C for 2h followed by 4°C for 4h.
3. Proceed to transformation of 1µl reaction mixture without purification.

B.5 PCR program for B7-H6 and PVR

Table B.3: *PCR program for T7EI.*

Stage	Temperature	Time	Cycles
Enzyme activation	95°C	10 min	1 X
Denature	95°C	30 sec	
Anneal	65°C (T _m)	30 sec	40X
Extend	72°C	1 min	
Final extension	72°C	7 min	1 X
Hold	4°C	Hold	1 X